UNIVERSITY OF CALIFORNIA
SANTA CRUZ

Wolbachia Localization and Transmission in *Drosophila* Oogenesis

A thesis submitted in partial satisfaction of the requirements for the degree of

MASTER OF SCIENCE

in

MOLECULAR, CELL AND DEVELOPMENTAL BIOLOGY

by

Yonah A. Radousky

December, 2022

The Thesis of Yonah Radousky is approved:

_____
Professor William Sullivan

_____
Professor Jordan Ward

_____
Professor John Tamkun

_____
Peter Biehl
Vice Provost and Dean of Graduate Studies

Table of Contents

List of Figures and Tables

Abstract

Wolbachia Localization and Transmission in *Drosophila* Oogenesis

Yonah Radousky

A broad array of endosymbionts ensure their spread through host populations via vertical transmission, yet much remains unknown concerning the type and number of cellular mechanisms underlying reliable transmission. *Wolbachia* are the most common endosymbionts in nature, but their prevalence varies greatly in host populations due to imperfect transmission. To better understand the cellular basis of *Wolbachia* transmission, this project explored the cellular distributions of *Wolbachia* diverged up to 40 million years in the oocytes of 18 divergent *Drosophila* species. This analysis revealed three cellular distributions: 1) a tight clustering of *Wolbachia* at the posterior pole plasm (the site of germline formation); 2) a concentration at the posterior pole plasm, but with a significant population of *Wolbachia* distributed throughout the oocyte; 3) and a distribution of *Wolbachia* throughout the oocyte, with none or very few located at the posterior pole plasm. Examination of this latter class reveal *Wolbachia* access the posterior pole plasm during the interval between late oogenesis and the blastoderm formation. *Wolbachia* in this class concentrate in the posterior somatic follicle cells that encompass the pole plasm of the developing oocyte suggesting these are the source of that ultimately occupy the germline. In contrast, strains in which *Wolbachia* concentrate in the posterior pole plasm, no or few

Wolbachia are found in the follicle cells associated with the pole plasm. Phylogenomic analysis indicates that closely related *Wolbachia* tend to exhibit similar patterns of posterior localization, suggesting that diverse localization strategies are a function of *Wolbachia*-associated factors. Previous studies revealed that endosymbionts rely on one of two distinct routes of vertical transmission: continuous maintenance in the germline (germline-to-germline) and a more circuitous route via the soma (germline-to-soma-to-germline). This work demonstrates that *Wolbachia* maintains the diverse arrays of cellular mechanisms necessary for both of these distinct transmission routes. This characteristic may account for its ability to infect and spread globally through a vast range of host insect species.

.

Dedication and Acknowledgments

I would like to thank Dr. William Sullivan for his consistent mentorship and unwavering passion for even the smallest discovery. I would like to thank Dr. Jordan Ward and Dr. John Tamkun for their role on the committee and feedback on the project. I would also like to thank all members of the Sullivan lab for making an amazing research environment and supporting my research. In addition, special thanks to Eliza Paneru and Cecilia Rugamas for being fantastic project members through all stages of my degree, as well as Sommer Fowler for her indispensable help and dissection skills. I would like to thank all the supportive members of my MCD cohort as well as the greater PBSE community. Finally, I would like to thank my parents and siblings and friend Heather for their constant support and advice through my time in graduate school.

The text of this thesis includes works of the following preprint material: Distinct Wolbachia localization patterns in oocytes of diverse Drosophila species reveal multiple strategies of vertical transmission, Yonah A. Radousky, Michael T.J. Hague, Sommer Fowler, Eliza Paneru, Adan Codina, Cecilia Rugamas, Grant Hartzog , Brandon S. Cooper, William T. Sullivan. The co-author William Sullivan listed in this publication directed and supervised the research which forms the basis for the thesis.

Section One: Background and Introduction

Wolbachia are widespread intracellular bacteria, estimated to be present in 30% to 60% of all insect species (Hilgenboecker et al., 2008). It is generally considered to be an endosymbiont, although it can display parasitic traits along with its mutualistic host interactions. Discovered in the early 1920s, it gained additional attention in the 1970s with the acknowledgment of *Wolbachia's* ability to promote cytoplasmic incompatibility in mosquitoes (Cowdry, 1923; Wolbach, 1924). Females infected with *Wolbachia* are able to have successful progeny after mating, but males crossed with uninfected females result in *Wolbachia*-induced cytoplasmic incompatibility (CI), dramatically reducing hatch rate. (Yen and Barr, 1971). CI, along with other bacterial effects on the host, has driven the rapid spread of *Wolbachia* through many insect populations.

In addition to its novel endosymbiotic characteristics, *Wolbachia* has also been associated with two distinct public health endeavors (Slatko et al., 2014). *Wolbachia* are obligate symbionts of filarial nematodes which are parasitic roundworms that cause lymphatic filariasis (severe welling in the lymph system) as well as onchocerciasis (river blindness). In these nematodes, *Wolbachia* is necessary for proper anterior-posterior determination in developing microfilaria (Landmann et al., 2014) As a result of this obligate relationship, antibiotics that target *Wolbachia* can deplete nematode replication by reducing the level of

successful progeny. Clinical study of this treatment method is ongoing as well as research into new drugs to target *Wolbachia* effectively (Hübner et al., 2020).

The *Wolbachia*-mosquito symbiotic relationship has also generated a great deal of interest by the biomedical community. When infected with *Wolbachia*, the mosquitos to ability to transmit certain viruses such as dengue fever, chikungununya fever, and yellow fever is reduced, in addition to some parasites and infectious protozoans (Bourtzis et al., 2013). This unique, but poorly understood relationship, offers a new strategy to prevent the spread of some insect borne viral diseases. *Aedes aegypti* mosquitoes are a main vector of dengue fever but are not naturally infected with *Wolbachia*. When infected with *Wolbachia* and released into populations where the virus is endemic, a reduction in the levels of dengue fever in the community was observed (Utarini et al., 2021).

The impact of *Wolbachia* infection with respect to the rate at which it spreads through a population and the suppression of viral replication varies greatly depending on the *Wolbachia* strain deployed. When testing was done with the *w*MelPop strain, it spread poorly through the uninfected mosquito populations (Nguyen et al, 2015; Turelli, 2010). Due to its less costly effects on insect viability, *w*Mel has become a more successful model of infection with the same ability of viral reduction. To date, successful introduction of *Wolbachia* into mosquito populations has resulted in significant reduction in the spread of dengue fever in some regions (Ryan et al., 2020; Tantowijoyo et al., 2020). In spite of these

successes, much remains unknown concerning the molecular and cellular mechanisms by which *Wolbachia* are vertically transmitted, spread through insect populations and suppress viral replication. As a natural host of *Wolbachia*, *Drosophila melanogaster* serves as an ideal model organism to investigate these issues.

This work focuses on understanding the mechanisms of *Wolbachia* vertical transmission. Vertical transmission though the maternal line is common among endosymbionts, and *Wolbachia* is a classic example of this route (Russell et al., 2019; Bright and Bulgheresi, 2010). In order to be inherited to the next generation, *w*Mel *Wolbachia* maintains an association with the future germline at critical stages of development. In *Drosophila* ovaries, multiple stages of egg development are simultaneously present. At the tip of each area is the region known as the germarium. This area contains germline stem cells which are actively dividing and undergoing cellular differentiation. During this early stage of egg development, *Wolbachia* can already be seen associated with the germline stem cells (Serbus et al., 2008). The differentiated cystoblast undergoes four rounds of mitotic divisions, resulting in sixteen interconnected cells. Of those sixteen, one becomes the nucleus of the oocyte and the other supporting nurse cells (Bastock and St. Johnston, 2008).

Early in oogenesis, *Wolbachia* are evenly distributed throughout all the cells in the chamber. Also at this stage, microtubules emanate from the oocyte into the nurse cells. By associating with the minus-end directed microtubule motor protein,

Wolbachia are transported from the nurse cells and concentrate at the anterior-end of the oocyte. As the oocyte matures, microtubules undergo a dramatic reorganization such that they originate from the oocyte cortex with their plus-ends oriented toward the posterior pole. This results in the release and dispersal of *Wolbachia* from the anterior pole. *Wolbachia* associate with the plus-end directed motor protein for transport to the posterior pole and the site of germline formation. Due to extensive cytoplasmic streaming, *Wolbachia* associate with pole plasm determinants to maintain their position at the site of germline formation (Sullivan, 2005).

Studying *Wolbachia* localization via confocal microscopy enables a convenient readout of the host factors with which *Wolbachia* engages throughout oogenesis. For example, the *Wolbachia* strain (*w*Riv) infecting *D. simulans* exhibits an initial anterior distribution, followed by a release from the anterior and becoming distributed across the entire mature oocyte. However, unlike the *w*Mel strain infecting *D. melanogaster*, it does not concentrate in the posterior pole (Veneti, Clark, Karr, Savakis, & Bourtzis, 2004) This suggests *w*Riv engages host Dynein and Kinesin, but not pole plasm determinants. *w*Mel *Wolbachia* strains introgressed into a *D. simulans* host exhibit a concentration in the pole plasm indicating the *Wolbachia* rather than the host drives oocyte localization properties. (Serbus & Sullivan, 2007)

Here, we examine vertical transmission routes and strategies across 40 million years of *Wolbachia* evolution in 18 *Drosophila* host species to gain a broader understanding of *Wolbachia* distribution and localization during host oogenesis. This approach provides a direct read-out of *Wolbachia* and host motor protein/pole plasm interactions that are highly conserved and those that vary between species. These studies complement and extend previous analysis that revealed *Wolbachia* strain-dependent localization patterns in the *Drosophila* embryo correlate with specific alleles of *wsp,* a major *Wolbachia* surface protein (Veneti *et al.,* 2004). We discovered three distinct *Wolbachia* distribution patterns in the oocyte: (1) the vast majority of *Wolbachia* clustered at the posterior pole; (2) a concentration at the posterior pole, but with a large portion of *Wolbachia* distributed throughout the entire oocyte; and (3) *Wolbachia* distributed throughout oocyte, with none or very few located at the posterior pole. This latter class is particularly interesting as it suggests *Wolbachia* must occupy the oocyte via a somatic route. We provide evidence that the neighboring somatic follicle cells are the likely source of germline *Wolbachia*.

Together, these findings indicate that *Wolbachia* are capable of achieving efficient vertical transmission either via strict maintenance in the germline from one generation to the next or via invasion of the germline through neighboring somatic cells. Thus, *Wolbachia* must maintain the diverse arrays of cellular mechanisms necessary for both of these distinct transmission routes. Phylogenomic analyses also demonstrate that *Wolbachia* abundance in the oocyte posterior region exhibits strong signal on the *Wolbachia* phylogeny, suggesting

localization patterns are determined by *Wolbachia*-associated factors. Further, this analysis identifies candidate surface proteins that may be responsible for these diverse localization patterns in host oocytes.

Results:

***Wolbachia* navigates the developing *Drosophila* oocyte in distinct stages**

Wolbachia pipientis localization pattern around the nucleus for *w*Mel has been documented before, but questions remain about its movement and positioning during oogenesis (Guo *et al.*, 2019; Kose and Karr, 1995; Ramalho *et al.*, 2018; Russell *et al.*, 2018b; Serbus *et al.*, 2008; Serbus and Sullivan, 2007; Veneti *et al.*, 2004). As a reference for further analysis of *Wolbachia* oocyte distributions in a range of *Drosophila* species, the key distribution patterns of *w*Mel throughout *D. melanogaster* oocytes are depicted in **Figure 1**.

Stage 1 includes the germarium, a structure consisting of the germline stem cells and their cystoblast daughter cells that will differentiate into a mature oocyte. Progression to stage 2, involves the cystoblast undergoing four rounds of mitotic division to produce a syncytium of 16 cells connected by cytoplasmic bridges and surrounded by a layer of somatically derived follicle cells (Bastock and St Johnston, 2008). Propidium Iodine (PI)-stained *Wolbachia* (red) are clearly observed as puncta in the cytoplasm of the infected, but not the uninfected 16 cell cyst (**Figure 1 Stages 1-2**). The actin is labeled in green.

Figure 1. Confocal micrographs of *D. melanogaster* oocytes tracked through early oogenesis. Samples stained with propidium iodide for DNA (red) and phalloidin (green) for actin. Representative stages of development (1-10) are shown for *Wolbachia* infected wild-type *D.mel* (left) and uninfected *D.mel* (right). Greyscale zoomed-in images around the nucleus of the oocyte are shown in the third column for both infected and uninfected flies, with arrows pointing to the *Wolbachia* at the nucleus. In stage 1-2 *Wolbachia* can be seen in the germarium, but nucleus size has yet to expand. By stage 3 there is an anterior localization around the expanded nucleus in which the *Wolbachia* appears to touch the membrane as outlined by the actin. This trend continues through stages 4 and 5 as the oocyte continues to expand. In stage 6 the number of follicle cells is increased, and *Wolbachia* titer appears to be reduced in the oocyte. By stage 7 the localization has shifted and *Wolbachia* can be seen throughout the oocyte and flowing down to the posterior pole as the cytoplasm of the oocyte is expanding rapidly. This shift continues through stage 8 with oocyte yolk now visible. At stage 9 anterior follicle cell migration occurs, and the *Wolbachia* already starts displaying an archlike posterior localization. During stage 10 of development oocyte volume takes up half the egg chamber and the posterior localization pattern becomes distinct. Red arrows track *Wolbachia* movement around the germline. Scale bars set at 15 μM.

Figure 1

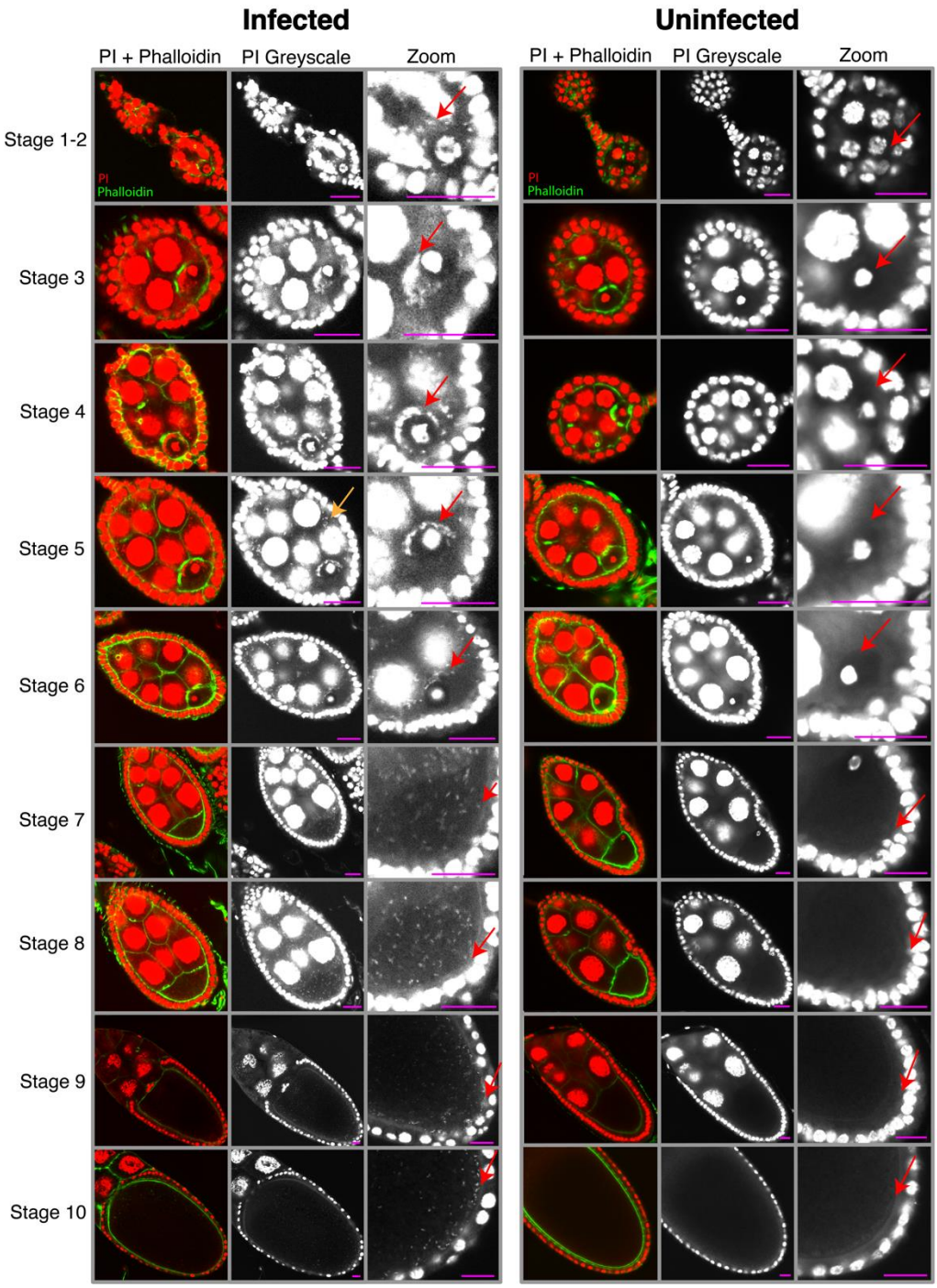
Infected
Uninfected
PI + Phalloidin
PI Greyscale
Zoom
PI + Phalloidin
PI Greyscale
Zoom
Stage 1-2
Stage 3
Stage 4
Stage 5
Stage 6
Stage 7
Stage 8
Stage 9
Stage 10
PI
Phalloidin
PI
Phalloidin

During stage 3, the cyst has become polarized with one of the cells differentiating into an oocyte and the others becoming polyploid nurse cells. *Wolbachia* are clearly seen in the infected oocyte cytoplasm anteriorly concentrated at two cytoplasmic bridges that connect to the nurse cells (**Figure 1, Stage 3**). Previous studies indicate that *Wolbachia* rely on the extensive complex of microtubules that radiate through the oocyte/nurse cell complex undergoing Dynein mediated transport to the anterior region of the oocyte (Ferree *et al.*, 2005).

During stages 4 and 5, the nurse cell/oocyte complex becomes oblong and is fully encapsulated by follicle cells. *Wolbachia* are clearly observed in both the oocyte and nurse cell cytoplasm (**Figure 1, Stages 4 and 5**). The *Wolbachia* in the oocyte are tightly associated with the anterior cortex.

During stage 6, the number of follicle cells increase and are more densely packed in a monolayer encompassing the oocyte. Here we discovered a previously unrecognized aspect of *Wolbachia* dynamics and localization. The number of anteriorly localized *Wolbachia* is greatly diminished at this stage (**Figure 1, Stage 6 and Figure 2**). Possibly *Wolbachia* in the oocyte are degraded or migrate through the ring canals back into the nurse cells (from whence they came). If the latter, it may be *Wolbachia* are prematurely engaging with host kinesin (see below).

Figure 2: Representative image of the reduction of *Wolbachia* titer between stages 4/5 and 6 in *D. melanogaster* oogenesis. *Wolbachia* stained with anti-FtsZ shown in pink. Scale bars set at 25 µM. (B) greyscale DAPI channel. (C) Greyscale of anti-FtsZ channel. (A'-C') 5X zoom around the nucleus of the oocyte during stage 4 shown for each channel. (A''-C") 4X zoom around the nucleus during stage 6 for each respective channel seen above. At least 10 oocytes across 3 slides were imaged with Z-stacks for a visual description of this trend.

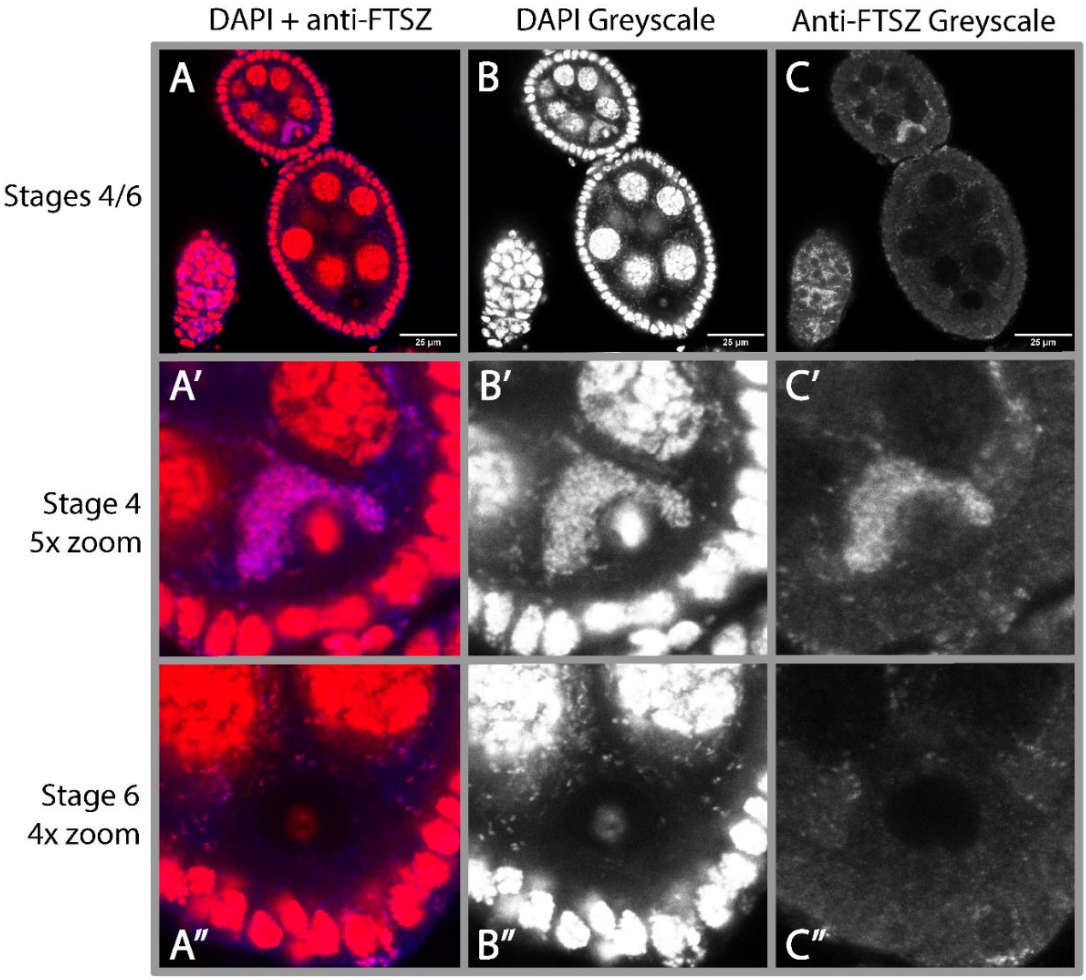

At stage 7, *Wolbachia* are again observed in the oocyte. However, rather than being tightly associated with the anterior cortex, *Wolbachia* are evenly distributed throughout the oocyte (**Figure 1, Stage 7**). Up through stage 6**,** the microtubules are organized with their minus-end located at the posterior pole of the oocyte with their plus-ends extending through the ring canals into the nurse cell complex (Mahowald and Strassheim, 1970). However, during stage 7 the microtubules reorient such that their plus-ends extend toward the posterior pole (Cha et al., 2001; Cha et al., 2002; Steinhauer and Kalderon, 2006). Accordingly, the plus-end motor protein kinesin is required to establish the even distribution of *Wolbachia* throughout the maturing oocyte (Serbus and Sullivan, 2007). Stage 8 heralds the beginning of vitellogenesis, the process of yolk formation and deposition of nutrients into the oocyte (Cummings et al., 1971). *Wolbachia* are near, but not yet located at, the posterior pole (**Figure 1, Stage 8**). At stage nine anterior follicle cell migration occurs (Rørth, 2002). At this stage, *Wolbachia* began displaying an archlike posterior cortical localization**. Figure 1, Stage 9**). By stage 10, the oocyte accounts for approximately half the volume of the egg chamber. Nurse cell dumping will shortly follow, leading into stage 11-12 with the oocyte rapidly growing in size (Mahajan-Miklos and Cooley, 1994). At stage 10, there is a distinct concentration of *Wolbachia* along the posterior cortex (**Figure 1, Stage 10**).

An initial concentration of *Wolbachia* at the oocyte anterior is a conserved feature in all *Drosophila* species examined.

As described above, *w*Mel *Wolbachia* enter the oocyte through a complex of ring canals connecting the nurse cells to the oocyte and concentrate at the anterior cortex. Initially observed in *D. melanogaster*, the number of *Wolbachia* increases dramatically while at the anterior (Ferree *et al.*, 2005). This concentration is at least in dpart due to import of *Wolbachia* from the nurse cells through the ring canals into the oocyte. The transport relies on the minus-end microtubule motor protein Dynein (Ferree *et al.*, 2005). The increase may also be a result of *Wolbachia* replication at this anterior site. To determine if anterior localization is a conserved aspect of *Wolbachia*'s navigation through the developing oocyte, we examined diverse *Wolbachia* strains in eight *Drosophila* species. As this analysis is technically difficult and labor intensive, it was impractical to examine all 18 species. However, these eight species span highly diverged *Wolbachia* strains and host species. As shown in **Figure 3**, all eight species analyzed exhibited a distinct anterior localization during mid-oogenesis. It is interesting that this localization occurs during stage 5 of oogenesis, which in *D. melanogaster* is prior to the localization of known anterior axis determinants. Thus, *Wolbachia* must be relying on as yet undiscovered anteriorly concentrated factor(s). The functional significance of this anterior localization remains unknown. Given the dramatic increase in *Wolbachia* abundance, the cytoplasmic environment of this anterior region may promote *Wolbachia* replication.

Figure 3. Conserved *Wolbachia* anterior localization during early oogenesis (stages 4-5). *Wolbachia* and host DNA stained with PI (red) and actin with phalloidin (green) shown in the left most column. Greyscale of PI channel shown in middle. 4X zoom-in around the oocyte shown on the right. All of the eight *Wolbachia* strains examined concentrate at the anterior cortex of the oocyte at this stage. Red arrows highlight *Wolbachia*'s anterior localization positioning (A) D. pandora, (B) *D. nikananu*, (C) *D. chauvacae*, (D) *D. simulans* (*w*Ha), (E) *D. curta*, (F) *D. bokci*, (G) *D. ananassae*, (H) *D. melanogaster*. Oocytes are approximately 50-75 μM in size.

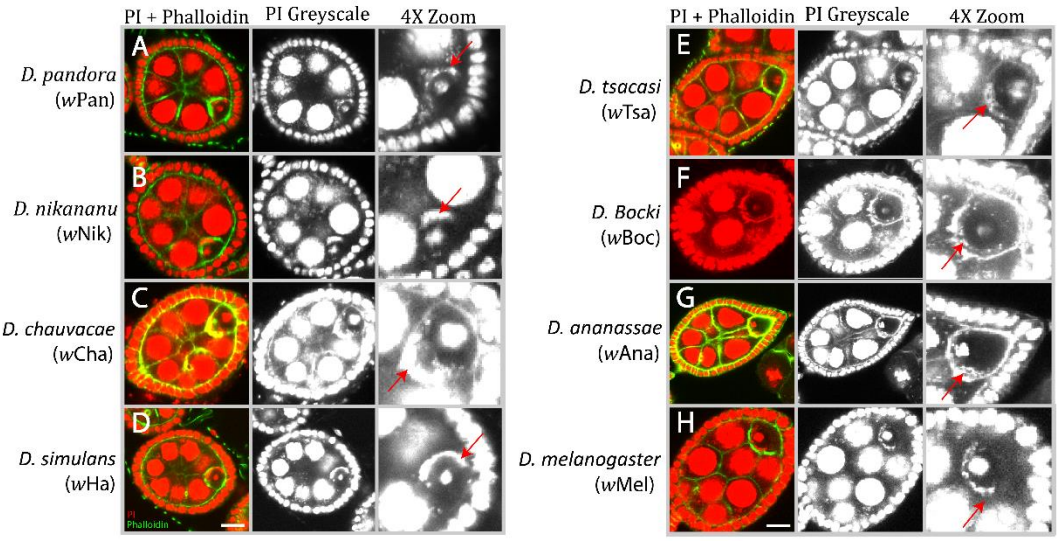

Wolbachia exhibits three distinct distributions with respect to posterior localization in the mature *Drosophila* oocyte

As described above, much is known concerning *Wolbachia* dynamics and localization patterns during oocyte development in *D. melanogaster*, as well as the host factors with which *Wolbachia* interacts (Serbus *et al.*, 2008). This thesis provides an outline of the molecular and cellular mechanisms driving *Wolbachia* vertical transmission. It also raises the question of whether the mechanisms and strategies observed in *D. melanogaster* are conserved across diverse *Wolbachia* strains and *Drosophila* species. To explore this issue, we examined 19 distinct *Wolbachia* strains. Estimated Bayesian phylograms depicting phylogenetic relationships among the *Wolbachia* strains and the *Drosophila* species are shown in **Figure 4**. Our analysis comprised 18 A-group *Wolbachia* strains, including six *w*Mel-like strains (Cooper et al., 2019; Hague et al., 2020a) and five *w*Ri-like strains (Turelli et al., 2018), as well as the B-group *Wolbachia* strain *w*Mau, which diverged from A-group *Wolbachia* up to 36 million years ago (Meany et al., 2019). These *Wolbachia* strains infect 18 divergent *Drosophila* host species spanning three species groups and up to 50 million years of evolution (Suvorov et al., 2022).

Figure 4. Bayesian phylograms depicting the evolutionary relationships among *Wolbachia* strains diverged up to 36 million years (left) and *Drosophila* host species diverged up to 50 million years (right). *w*Mel- and *w*Ri-like clades of closely related *Wolbachia* are labeled on the left. Gray lines pair *Wolbachia* strains with their *Drosophila* host species, which highlights patterns of topological discordance due to introgressive and horizontal transfer of *Wolbachia* among host species. The *Wolbachia* phylogram was estimated using 66 full-length and single-copy genes (43,275 bp) of equal length. The host phylogram was estimated using 20 conserved single-copy genes (see Methods). All nodes have posterior probabilities >0.95. *Wolbachia* and host divergence times in millions of years (MYA) are reproduced from Meany et al. (2019) and Suvorov et al. (2022), respectively.

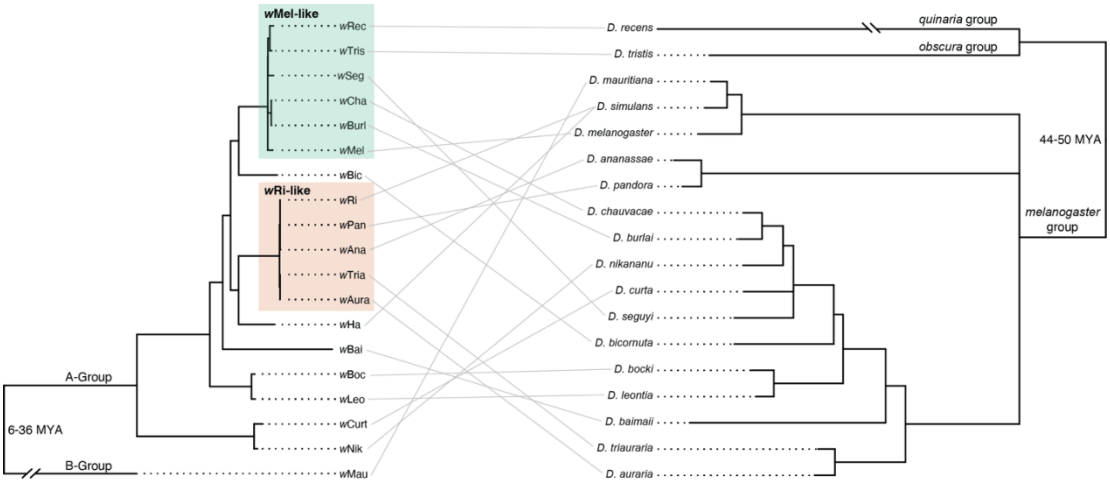

In *D. melanogaster*, oocyte microtubules undergo a dramatic rearrangement during stages 7 – 8 of mid-oogenesis (Theurkauf *et al.*, 1992). Microtubule minus-ends, originally concentrated at the posterior pole with their plus-ends extending anteriorly through the ring canals, reorganize such that the microtubule minus ends orient toward anteriorly. Concomitant with this microtubule rearrangement is the release of *w*Mel *Wolbachia* from the oocyte anterior resulting in the dispersal of the bacteria throughout the entire length of the oocyte with a fraction concentrating at the posterior pole (Ferree *et al.*, 2005). The posterior dispersal of *Wolbachia* requires the plus-end motor protein kinesin (Serbus and Sullivan, 2007). Maintenance of those *Wolbachia* that reach the posterior pole rely on a stable association with key pole plasm components (Serbus et al., 2011).

We examined the oocytes of 18 *Drosophila* species (N = 72 total oocytes) infected with 19 diverse *Wolbachia* strains to determine whether there is variability in its oocyte posterior distribution. Unlike the conserved anterior localization, *Wolbachia* exhibited three distinct patterns of posterior localization. As shown in **Figure 5** and **Figure 6,** eight *Drosophila* species exhibited a *Wolbachia* localization pattern similar to that observed for *D. melanogaster* with the bulk of *Wolbachia* evenly distributed throughout the oocyte and a significant fraction concentrated at the posterior pole ("*D.mel*-like" or "posteriorly localized").

Figure 5. Three distinct patterns of posterior *Wolbachia* localization during late stage oogenesis (A-C). Confocal micrographs of *Drosophila* oocytes DNA-stained with PI (red) and actin-stained with phalloidin. (green) show representative examples of (A) Posterior localization in *D. tristis*, (B) clumped in *D. bicornuta*, and (C) dispersed localization in *D. triauraria*. (A'-C') depicts single channel images of PI staining. (A"-C") depicts an enlarged PI-stained image of the posterior region of each oocyte. Scale bars set at 25 μM.

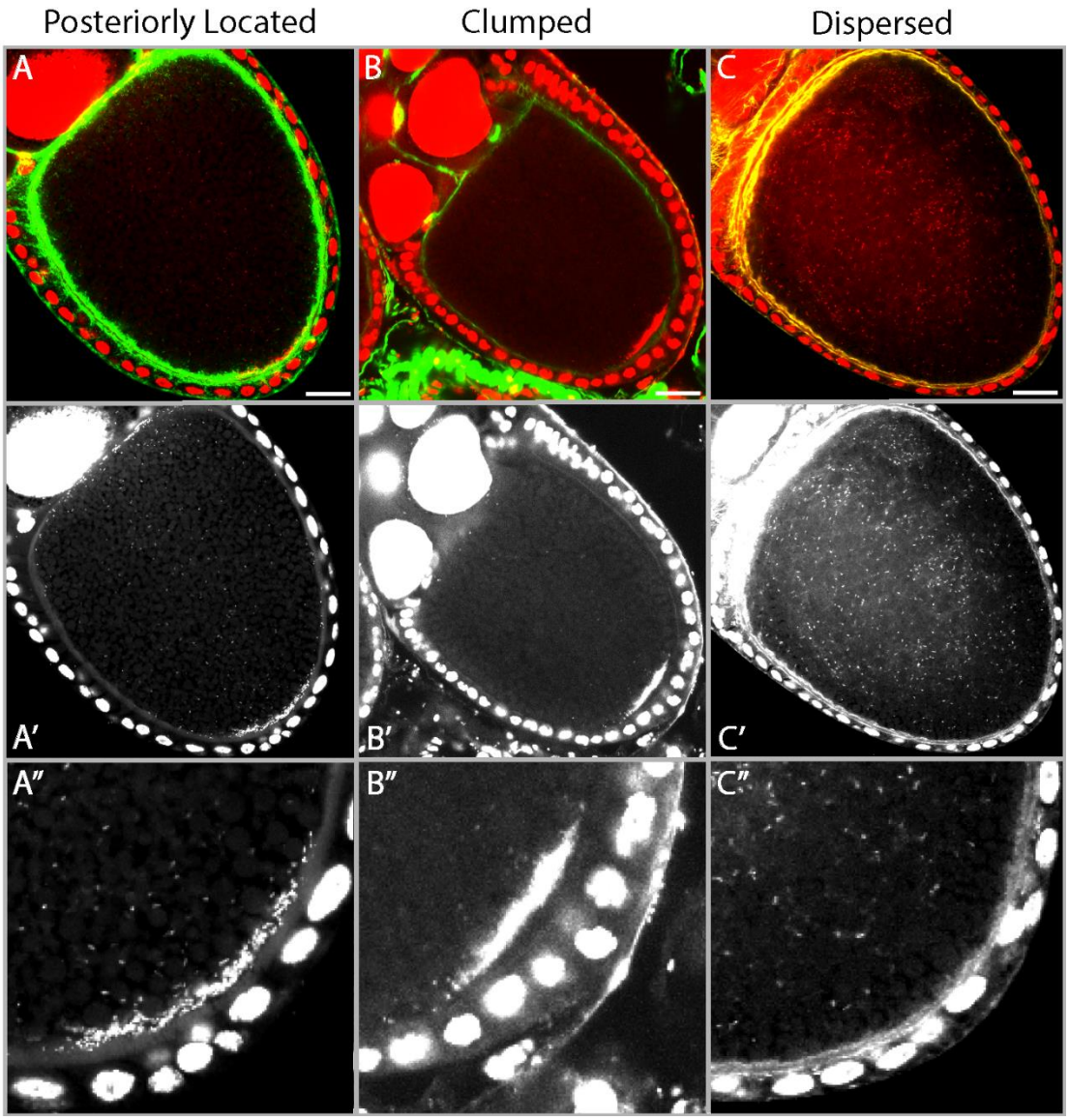

Figure 6. Representative images of posteriorly localized *Wolbachia*. Confocal micrographs of *Drosophila* oocytes DNA-stained with PI (red) and actin-stained with phalloidin (green) show representative examples of infected *Drosophila* species with posteriorly localized *Wolbachia*. Second row depicts single greyscale channel images of PI staining. Third row depicts a enlarged PI-stained image of the posterior region of each oocyte. Scale bar set at 25 µM.

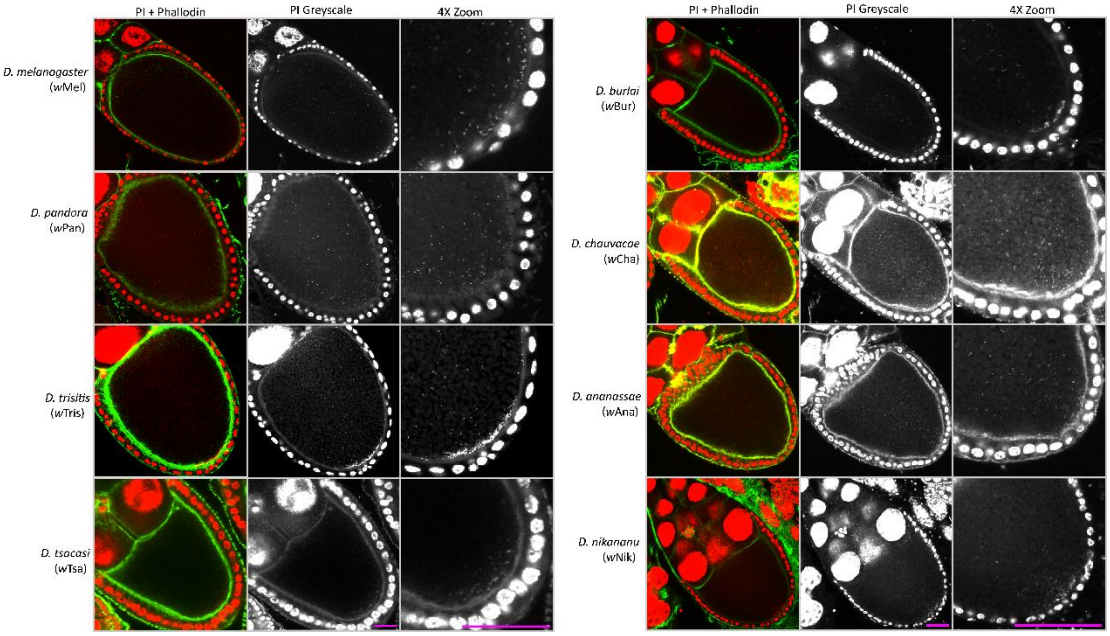

Our analysis revealed four *Drosophila* species manifested a second pattern in which the vast majority of *Wolbachia* localized a distinct cluster at the posterior pole and only small amounts of *Wolbachia* are distributed throughout the remainder of the oocyte **(Figure 7)**. In contrast to the pattern described above, rather than being distributed in a wide arc along the posterior pole, they are tightly centered at the extreme posterior region of the oocyte (**Figure 5B**). We have termed this pattern "Posteriorly clumped".

Figure 7. Representative images of posteriorly clumped *Wolbachia*. Confocal micrographs of *Drosophila* oocytes DNA-stained with PI (red) and actin-stained with phalloidin (green) show representative examples of infected *Drosophila* species with posteriorly localized *Wolbachia*. Second row depicts single greyscale channel images of PI staining. Third row depicts an enlarged PI-stained image of the posterior region of each oocyte. Scale bar set at 25 μM.

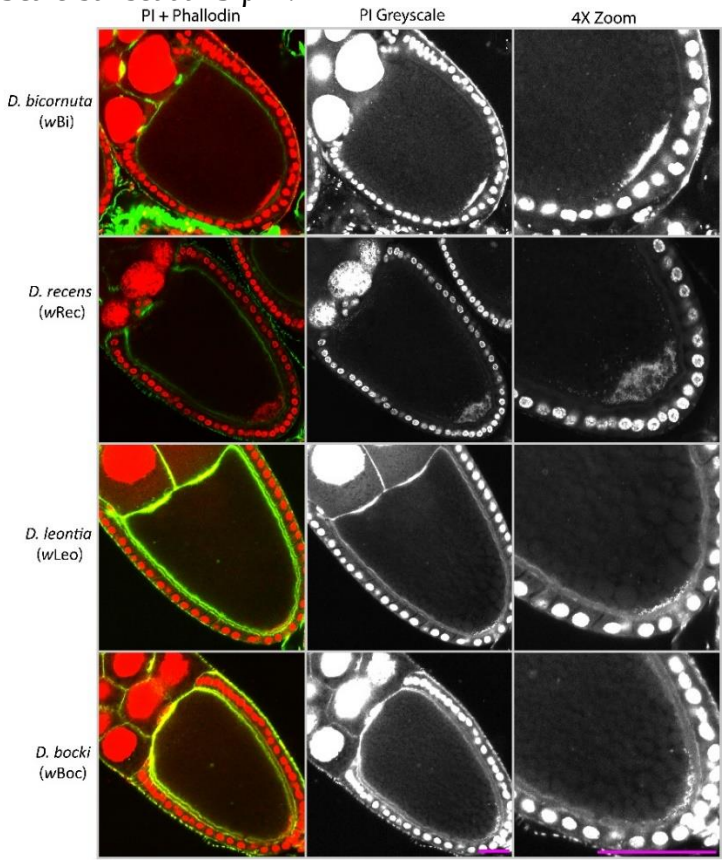

Finally, six *Drosophila* species exhibited a third pattern in which *Wolbachia* are distributed throughout the entire oocyte but few to none are localized at the posterior pole (**Figure 5C and Figure 8).** While there may be one to a few *Wolbachia* in this region, this pattern is likely due to the random nature of the distribution rather than a targeted localization. The lack of the *Wolbachia* at the posterior pole was unexpected as this was thought to be necessary for incorporation into the germline of the next generation. We have termed this pattern "Dispersed". The species found in each of the three posterior localization patterns are summarized in **Table 1.**

Figure 8. Representative images of dispersed *Wolbachia*. Confocal micrographs of *Drosophila* oocytes DNA-stained with PI (red) and actin-stained with phalloidin (green) show representative examples of infected *Drosophila* species with posteriorly localized *Wolbachia*. Second row depicts single greyscale channel images of PI staining. Third row depicts a enlarged PI-stained image of the posterior region of each oocyte. Scale bar set at 25 μM.

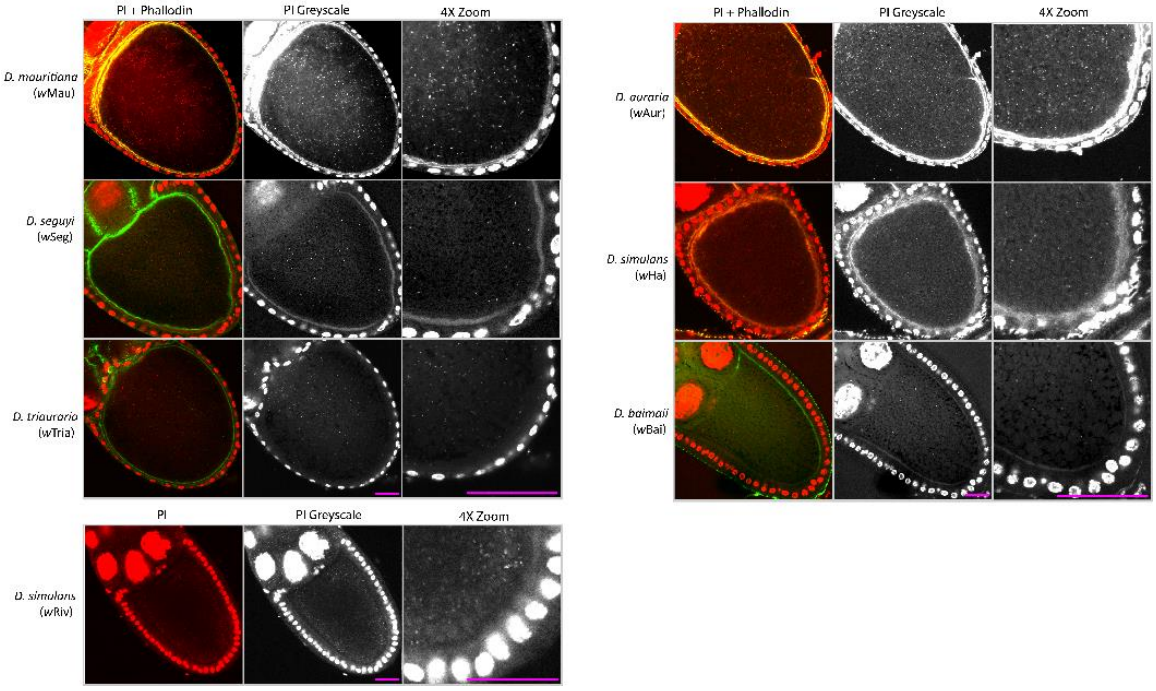

Table 1. Qualitative and quantitative quantification of cellular *Wolbachia* abundance and localization in stage 10 oocytes. The number of confocal images (*N*) used to generate means is shown for each *Wolbachia*-infected host species.

***Wolbachia* strain**	**Host species**	**Phenotype**	***N***	**Whole oocyte mean CTCF**	**Posterior mean CTCF**	**Pole mean CTCF**
*w*Rec	*D. recens*	clumped	3	482173.997	300752.607	58452.6233
*w*Tris	*D. tristis*	localized	4	223048.245	129013.48	105641.393
*w*Seg	*D. seguyi*	dispersed	5	58551.838	11402.24	557.266
*w*Cha	*D. chauvacae*	localized	5	108588.462	42635.702	9786.312
*w*Burl	*D. burlai*	localized	4	72805.8475	53754.31	36944.0925
*w*Mel	*D. melanogaster*	localized	2	191450.995	136174.465	92341.025
*w*Bic	*D. bicornuta*	clumped	3	90114.1267	83620.5133	54900.0233
*w*Ri	*D. simulans*	dispersed	5	333504.623	90663.7628	20493.8647
*w*Pan	*D. pandora*	localized	3	45422.88	6485.59333	1889.51667
*w*Ana	*D. ananassae*	localized	4	41577.575	16842.655	12927.14
*w*Tria	*D. triauraria*	dispersed	2	487897.4	1809.345	345.03
*w*Aura	*D. auraria*	dispersed	5	266477.962	3698.914	645.122
*w*Ha	*D. simulans*	dispersed	5	82940.852	3487.698	806.636
*w*Bai	*D. baimaii*	dispersed	2	11359.025	0	0
*w*Boc	*D. bocki*	clumped	6	137664.443	98338.8983	82408.17
*w*Leo	*D. leontia*	clumped	4	997045.048	685260.053	713918.118
*w*Curt	*D. curta*	localized	4	61314.02	36478.0175	20619.52
*w*Nik	*D. nikananu*	localized	3	44763.6567	27099.45	13013.73
*w*Mau	*D. mauritiana*	dispersed	3	69361.82	798.613333	321.866667

*CTCF = Corrected total cell fluorescence

Quantification of the three patterns of *Wolbachia* oocyte distribution

This work establishes three distinct classes (posteriorly localized, posteriorly clumped, and dispersed) that qualitatively describe different *Wolbachia* localization patterns in host oocytes. We used one-way ANOVAs to test whether these three classes differ statistically in quantitative estimates of *Wolbachia* abundance in the whole oocyte, at the posterior region, and at the posterior cortex (**Figure 9**). We defined the posterior region as the posterior 12.5% of the oocyte and the posterior cortex as the narrow region of oocyte where poll cells are located, then measured total *Wolbachia* abundance in each region as the corrected total cell fluorescence (CTCF). We found that the three classes have significantly different levels of *Wolbachia* abundance in whole oocytes (one-way ANOVA, $F_{(2,69)} = 6.2$, $P = 0.003$). Post-hoc comparisons indicate that the clumped group has significantly more *Wolbachia* in whole oocytes than the localized group ($P = 0.002$). The three groups also differed significantly in the amount of *Wolbachia* in the posterior region ($F_{(2,69)} = 23.09$, $P < 0.001$), such that the dispersed group has significantly less *Wolbachia* at the posterior that the clumped ($P < 0.001$) and localized ($P < 0.001$) groups. Finally, the three groups also differ in the amount of *Wolbachia* at the posterior cortex ($F_{(2,64)} = 38.12$, $P < 0.001$). Here, post-hoc comparisons indicate that all three groups significantly differ in levels of *Wolbachia* at the posterior cortex: the clumped group has the most *Wolbachia*, followed by localized, and then dispersed (**Figure 9**). Mean estimates of *Wolbachia* abundance (CTCF) for each *Wolbachia* strain and host species are shown in **Table 1**.

Figure 9 Cellular *Wolbachia* abundance in stage 10 oocytes measured as *Wolbachia* fluorescence due to propidium iodide (CTCF). Points are color coded by *Wolbachia* localization pattern (clumped, localized, dispersed), with unique shapes indicating each *Wolbachia* strain and host species. Asterisks indicate significant differences among groups based on one-way ANOVAs and post-hoc comparisons based on *P*-values <0.05 adjusted for multiple comparisons. Above, a schematic is shown for fluorescent quantification of different regions of the oocyte using the PI greyscale channel: the whole oocyte, the posterior region, and the posterior cortex.

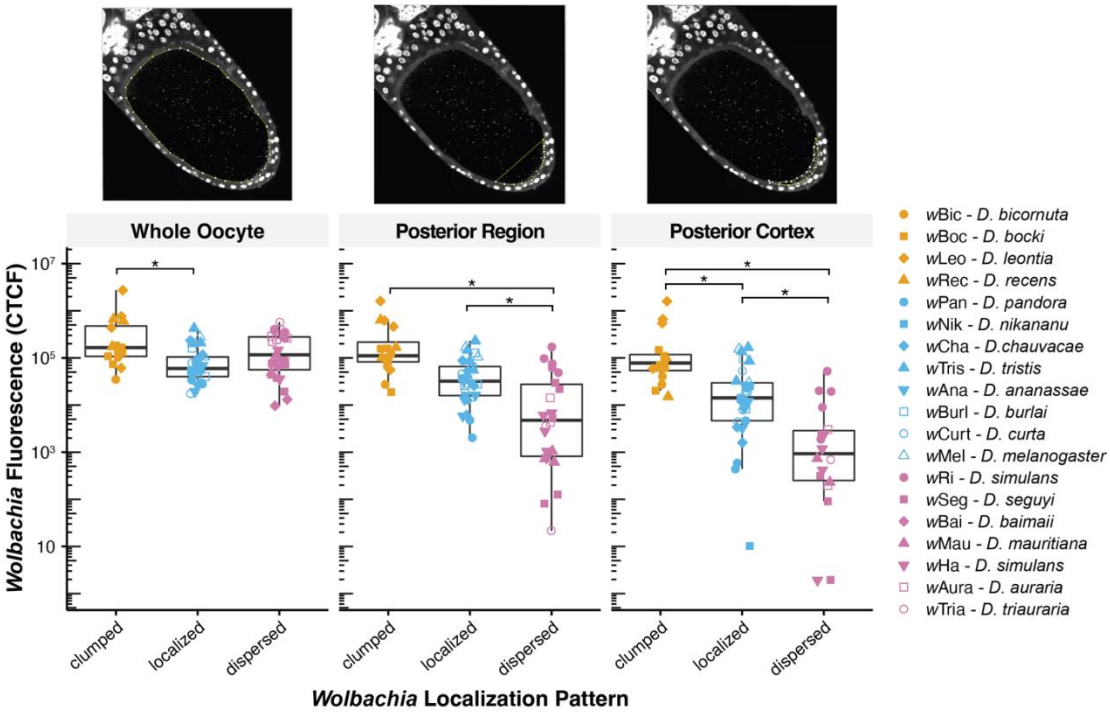

Wolbachia abundance in the oocyte posterior has strong phylogenetic signal

We hypothesized that the diversity of *Wolbachia* localization patterns may be due to *Wolbachia*-associated factors, such that closely related *Wolbachia* strains exhibit similar localization patterns in host oocytes. We used our phylogram describing the evolutionary relationships among *Wolbachia* strains to test whether patterns of *Wolbachia* localization exhibit phylogenetic signal using Pagel's λ (Hague *et al.*, 2020b; Hague et al., 2021; Pagel, 1999) (**Figure 10**)**.** A λ value of 1 is consistent with character evolution, a measure of a trait changing along an evolutionary tree, that entirely agrees with the *Wolbachia* phylogeny (i.e., strong phylogenetic signal). Whereas a value of 0 indicates that character evolution occurs independently of phylogenetic relationships (Freckleton et al., 2002; Pagel, 1999). Most notably, we found that *Wolbachia* abundance (CTCF) in the posterior region exhibits strong, significant phylogenetic signal (λ = 0.982 [0, 0.998], $P = 0.021$). *Wolbachia* abundance at the posterior cortex also has a high, but non-significant λ value (λ = 0.959 [0, 0.995], $P = 0.683$). Here, the large confidence intervals and our simulations suggest that a larger *Wolbachia* phylogeny ($N = 25$, 50 *Wolbachia* strains) is required to detect a significant signal of λ > 0 (**Figure 11)**. These results highlight differences in patterns of *Wolbachia* localization between the *w*Mel- and *w*Ri-like *Wolbachia* clades (**Figure 10**). Closely related *w*Mel-like *Wolbachia* tend to occur at a higher abundance in the posterior region of oocytes, whereas the *w*Ri-like strains are generally more dispersed. We found no evidence that *Wolbachia* abundance in the whole oocyte exhibits phylogenetic signal. (λ < 0.001 [0, 0.753], $P = 1$).

Figure 10. A) Estimated Bayesian phylogram for the 19 A- and B-group *Wolbachia* strains included in tests for phylogenetic signal. Divergence time (MYA) is superimposed from Meany et al. (2019). **B)** Mean estimates of *Wolbachia* fluorescence (log-transformed CTCF) in the whole oocyte, posterior region, and the posterior cortex. *Wolbachia* fluorescence in the posterior region has significant phylogenetic signal (λ = 0.982 [0, 0.998], P = 0.021), suggesting *Wolbachia*-associated factors determine *Wolbachia* abundance in the oocyte posterior. **C)** Estimated Bayesian gene tree of *Wolbachia* surface protein *WD1085*. *Wolbachia* fluorescence at the posterior region (λ = 0.974 [0, 0.998], P = 0.001) and the posterior cortex (λ = 0.942 [0, 0.994], P = 0.028) exhibit especially strong phylogenetic signal on the *WD1085* gene tree. All nodes have posterior probabilities >0.95.

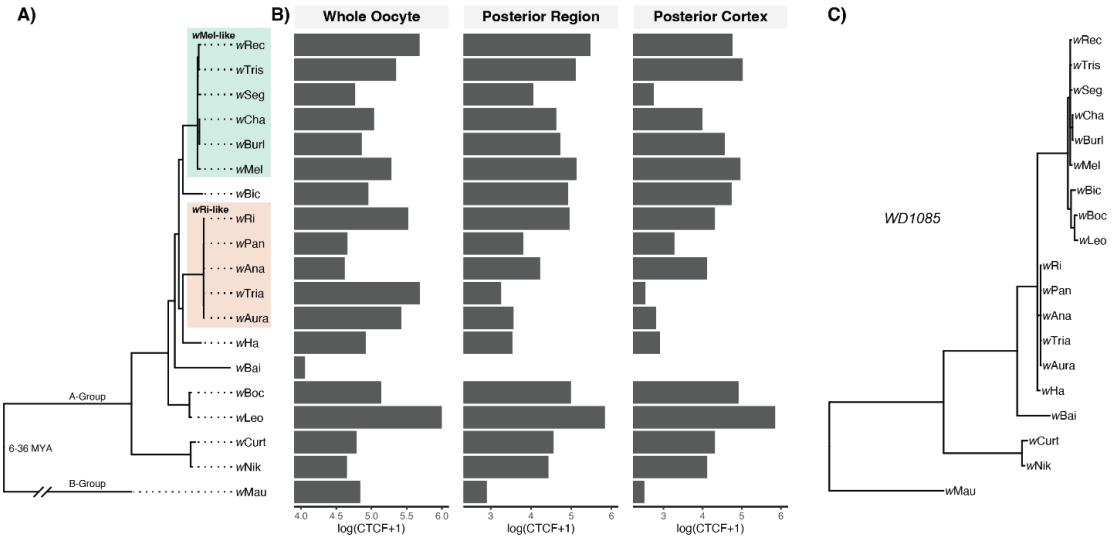

Figure 11. Distribution of maximum likelihood estimates of λ from 1,000 bootstrap replicates based on the *Wolbachia* phylogram and *Wolbachia* fluorescence at the oocyte posterior cortex (log-transformed CTCF). The bootstrap analysis of our *Wolbachia* phylogram is shown to the left (N = 19 *Wolbachia* strains). To the right are simulated phylogenies with an increasing number of *Wolbachia* strains included (N = 25, 50). For simulated trees, character evolution was simulated with our λ estimate of 0.959 using the "sim.bdtree" and "sim.char" functions in the *Geiger* R package (Harmon et al. 2008). For each graph, fitted λ values for the original phylogeny are shown above with a vertical dashed line. Note that fitted λ values for the simulated phylogenies differ slightly from λ = 0.959, because "sim.char" uses a Brownian-motion model to simulate character evolution along the phylogeny. Below each graph, the mean estimate of λ from the 1,000 replicates ($\overline{\lambda}$) is shown with associated 95% confidence intervals. Small phylogenies (e.g., N = 19) are likely to generate many near-zero λ values by chance, not necessarily because the phylogeny is unimportant for trait evolution (Boettiger et al. 2012). As the number of strains in our analysis increases (N = 25, 50), bootstrapped estimates of λ cluster around the true λ value fitted to the original phylogeny.

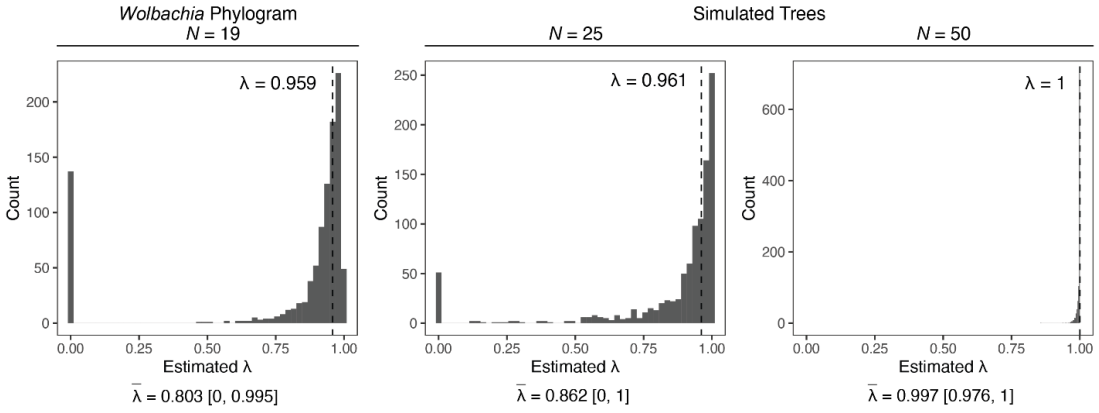

The correlation between *Wolbachia* localization in oocytes and phylogenetic divergence implies that factors in the *Wolbachia* genome determine *Wolbachia* concentration at the oocyte posterior. Because these distributions likely involve direct interactions between *Wolbachia* and the host cytoplasm, we focused on six major *Wolbachia* surface proteins (*wsp* (WD1063), *wspB* (WD0009), *wspC* (WD0489), WD0501, WD1041, WD1085) and tested whether sequence divergence at any of these candidate loci predicts *Wolbachia* localization patterns. Specifically, we tested whether gene trees of the *Wolbachia* surface proteins (**Figure 12**) exhibit phylogenetic signal, using the methods described above. One surface protein (WD1085) stood out with especially strong evidence of phylogenetic signal, which included significant departures from $\lambda = 0$ for *Wolbachia* abundance at the posterior region ($\lambda = 0.974$ [0, 0.998], $P = 0.001$) and the posterior cortex ($\lambda = 0.942$ [0, 0.994], $P = 0.028$) (**Figure 11C**). In addition, *Wolbachia* abundance at the posterior region also exhibited significant phylogenetic signal on the gene tree of WD0501 ($\lambda = 0.992$ [0.521, 1], $P = 0.022$). All tests for phylogenetic signal using *Wolbachia* gene trees are summarized in **Table 2**.

We recently found that the surface protein *wspB* is pseudogenized in a tropical variant of *w*Mel due to a premature stop codon, which seems to influence *w*Mel abundance in stage 10 oocytes when hosts are reared in the cold (Hague *et al.*, 2022). Here, we did not find that the *wspB* gene tree exhibits phylogenetic signal related to *Wolbachia* oocyte abundance (**Table 2**); however, we note that *wspB* appears to be psuedogenized in a number of other *Wolbachia* strains in addition to *w*Mel.

Figure 12. Gene trees of *Wolbachia* surface proteins. All nodes have Bayesian posterior probabilities of > 0.95 unless otherwise noted (see only *wspC*).

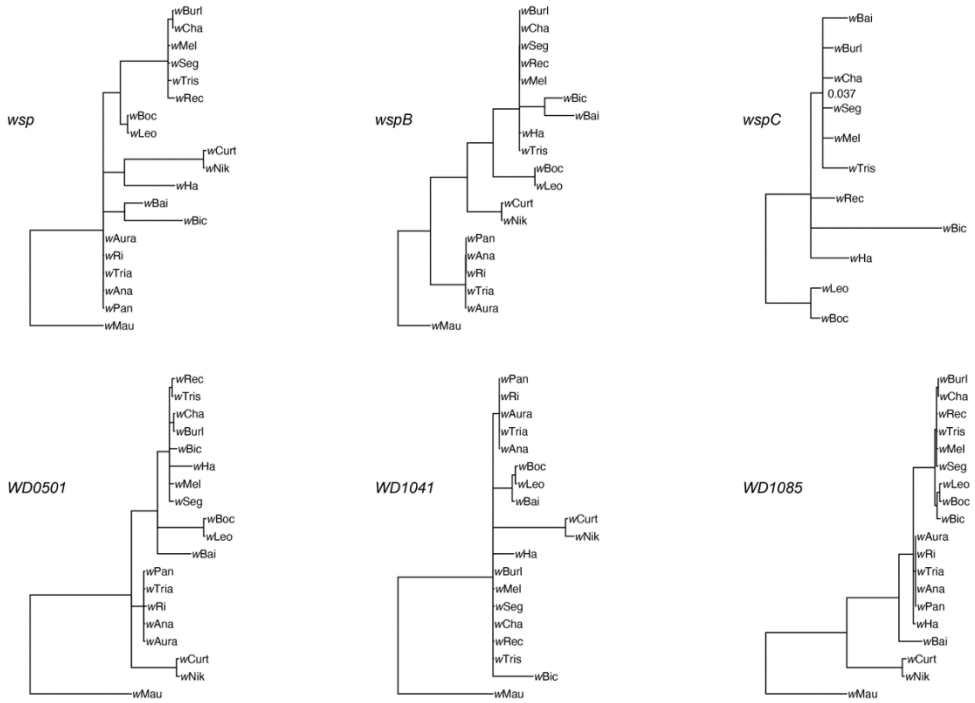

Table 2: Estimates of phylogenetic signal (Pagel's λ) with 95% confidence intervals (CI) for *Wolbachia* surface proteins.

Locus	Whole Oocyte				Posterior Region				Posterior Cortex			
	λ	**Lower CI**	**Upper CI**	***P***	**λ**	**Lower CI**	**Upper CI**	***P***	**λ**	**Lower CI**	**Upper CI**	***P***
wsp	0.000	0.000	0.578	1.000	0.945	0.000	0.993	0.071	0.000	0.000	0.633	1.000
wspB	0.000	0.000	0.401	1.000	0.000	0.000	0.374	1.000	0.279	0.000	0.720	0.655
wspC	0.210	0.000	0.947	0.659	0.000	0.000	0.845	1.000	0.000	0.000	0.811	1.000
WD0501	0.000	0.000	0.597	1.000	0.992	0.521	1.000	0.022	0.000	0.000	0.536	1.000
WD1041	0.000	0.000	0.692	1.000	0.000	0.000	0.555	1.000	0.000	0.000	0.484	1.000
WD1085	0.000	0.000	0.553	1.000	0.974	0.000	0.998	0.001	0.942	0.000	0.994	0.028

We found derived deletions of varying length in the *wspB* sequences of *w*Ha and *w*Bai beginning at nucleotide position 256, both of which produce frame shifts that generate multiple downstream stop codons (**Figure 13**). In addition, *w*Boc and *w*Leo share a large insertion starting at bp position 351. Because the insertions contain a contig break, we were unable to resolve the full length of the insertion. Lastly, *w*Bic contains a 104 bp insertion at bp position 647 that creates multiple downstream stop codons. These results suggest that the surface protein *wspB* has become psuedogenized at least four times in different *Wolbachia* lineages. Notably, the *Wolbachia* strains with a putatively pseudogenized version of *wspB* do not differ from the other strains in mean *Wolbachia* abundance in whole oocytes (Wilcoxon rank sum test, $W = 36$, $P = 0.964$), the posterior region ($W = 37$, $P = 0.893$), or the posterior cortex ($W = 41$, $P = 0.622$). This suggests that psuedogenization of *wspB* does not influence the diverse patterns of *Wolbachia* localization observed here.

Figure 13. Full amino acid alignment of *WspB* homologs in *w*Mel and the *Wolbachia* strains with a pseudogenized version of the surface protein. Stop codons are indicated by asterisks and insertions of varying length are indicated by “XXX”.

```
wMel_reference      MISKKTLAVTAFALLLSQQSFASETEGFYFGSGYYGQYLNNTSVLKTSTTGIKNLSINDR   60
wHa                 MISKKTLAVTAFALLLSQQSFASETEGFYFGSRYYGQYLNNTSVLKTSTTGIKNLSINDR   60
wBai                MISKKTLAVTALALLLSQQSFASETEGFYFGSGYYGQFFNGMGELKTSTTDIKNLSINDR   60
wBoc                MISKKTLAVTALALLLSQQSFASETEGFYFGSGYYGQFFNGMGELKTSTTDIKNLSINDR   60
wLeo                MISKKTLAVTALALLLSQQSFASETEGFYFGSGYYGQFFNGMGELKTSTTDIKNLSINDR   60
wBic                MISKKTLAVTAFALLLSQQSFASETEGFYFGSGYYGQYLNNTSVLKTSTTGIKNLSINDR   60

wMel_reference      GAQNTEGQSLSEYKGDYNPPFAANVAFGYTGELGNNSYRAELEGMYSSVKVD---NIGLT  117
wHa                 GAQNTEGQSLSEYKGDYNPPLLQMWHLVTQENWVTTAIGLNWKGCILL*KWI---ILV*Q  117
wBai                DAQNTKGQSLSEYKGDYNPPL------VIQGNWVTTAIGLNWKGCILL*KWI---ILV*Q  111
wBoc                GAQNTKGQSLSKYKGDYNPPFAANVALGYTGELGNNSCRAELEGMYSSVKVDXXXILV*Q  120
wLeo                GAQNTKGQSLSKYKGDYNPPFAANVALGYTGELGNNSCRAELEGMYSSVKVDXXXILV*Q  120
wBic                GAQNTEGQSLSEYKGDYNPPFAANVAFGYTGELGNNSYRAELEGMYSSVKVD---NIGLT  117

wMel_reference      SSQITVSYLKETGEDPDKETYLYSAAVSHDQIENISVMANVYHHWKSDRFSFSPYVGIGI  177
wHa                 VAK*LFHT*RRLVRILIKKLISIVLQLVMTKLRTYL*WQMFIIIGKVTVSLFLLTLVLGS  177
wBai                VAK*LFHI*RTLVRMLIKKLISIVLQLIMTKLRTYL*WQMFIIIGKVTVSLFLLTLVLES  171
wBoc                VVK*LFHT*RTLVRMLVKKLVSIVLQLIMTKLKTCL*WQMFIIIGRVTVSLFLLMLGLES  180
wLeo                VVK*LFHT*RTLVRMLVKKLVSIVLQLIMTKLKTCL*WQMFIIIGRVTVSLFLLMLGLES  180
wBic                SSQITVSYLKETGEDPNKETYLYSAAVSHDQIENISVMANVYHNWKSDRFSFSPYVGIGI  177

wMel_reference      GATRMTMFEKPSIRPAGQLKAGFDYRINEDVN---MHIGYRGFGAIGSDIKLTAKRLGQV  234
wHa                 VQQE*RCLKNRQ*DPQVN*KLALTIA*TKM*I---CISDIEVLVLLVAILSLQQKG*DKW  234
wBai                VQQE*RCLKNRQ*DPQVK*KLALTIT*TKM*I---CISDIEVLVLLVAILSLQQKS*DKW  228
wBoc                VQQE*QCLKNRQ*DPQVN*KLALIIT*TKM*I---CISDIEVLVLLVVLLVMVLNLQRMR  237
wLeo                VQQE*QCLKNRQ*DPQVN*KLALIIT*TKM*I---CISDIEVLVLLVVLLVMVLNLQRMR  237
wBic                GATRMTMFEKPSIRPAGQLKAGFDYRINEDV*XXXCISDIEVLVLLVAILSLQQKG*DKW  237

wMel_reference      VDDPNNDKKKK------LNPSSGSKVTEEINIGNQLFHTHGIEAGLTFHFASKA        282
wHa                 *TTLIMIKKRS------LILAQVAK*LRK*I*VINYFIHTV*RLVLLSILPAKL        282
wBai                *TTLIMIKKRS------LILAQVAKYSISHNSPNRS*EGRINSTTKGFE*RNV-        275
wBoc                LEKL*MILITGIKRSLMIRVNQQMQQKKI*I*VIHRFTHTV*RLALLSTLPAKL        291
wLeo                LEKL*MILITGIKRSLMIRVNQQMQQKKI*I*VIHRFTHTV*RLALLSTLPAKL        291
wBic                *TTLIMIKKRS------LILAQVAKYSTSRNSPNRIRYVLMAMVEQ*HIMICSD        285
```

To gain insight into their cellular function, we placed *wsp1085*, *wsp*, *wspB* and WD0501 in a yeast expression vector and assayed for growth inhibition (Siggers and Lesser, 2008). Using this system, we found that expression of a number of *Wolbachia* genes significantly inhibited *Wolbachia* growth in yeast **(Figure 14)**. However ectopic expression in yeast of the four wsp genes above produced no obvious effect on growth (**Table 3**). Whether this is due to inadequate expression levels or due to these surface proteins interacting with cellular components unique to the *Drosophila* oocyte remains to be determined.

Figure 14
To gain insight into WD_0501 (RS0225/p44/Msp2) and WD_1085 (RS04910/bamA) cellular function, we ectopically expressed these genes in yeast using a Galactose inducible promoter. Under normal growth conditions, ectopic expression of both genes inhibited growth, with WD_1085 (RS04910/bamA) exhibiting a more pronounced inhibition. Growth inhibition of WD_1085 was dramatically increased when the integrity of microtubules was compromised with the yeast placed in the mad1 spindle assembly checkpoint background or the microtubules were compromised directly through the addition of benomyl. These results suggest that WD_1085 may directly or indirectly interact with host microtubules.

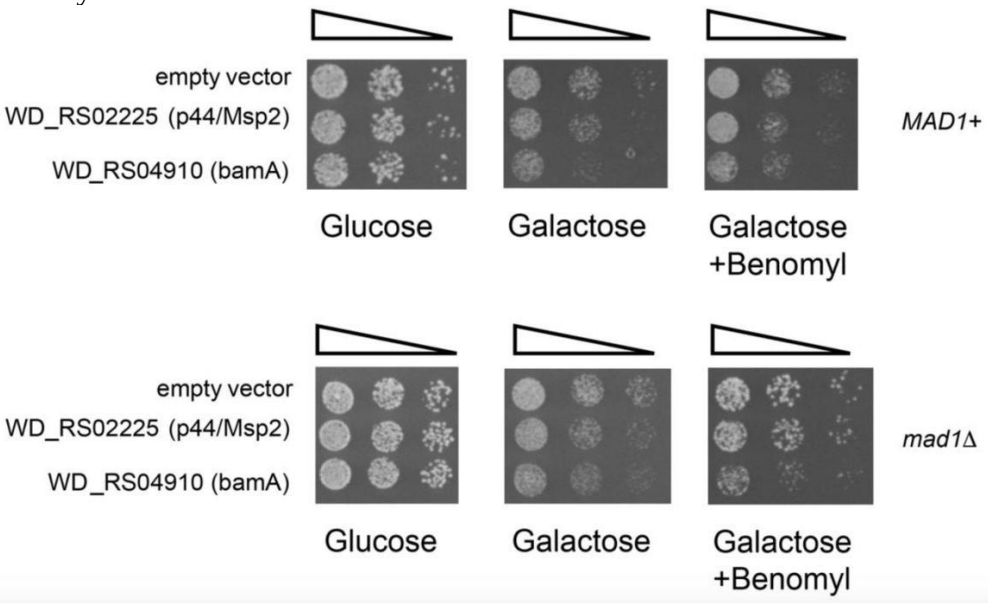

Lastly, we ran similar phylogenetic analyses using the host phylogeny (as opposed to *Wolbachia*) to test whether host-associated factors might also contribute to diversity patterns of *Wolbachia* (**Figure 15**). We found no evidence that total *Wolbachia* abundance in whole oocytes ($\lambda < 0.001$ [0, 0.685], $P = 1$) or the posterior cortex ($\lambda < 0.001$ [0, 0.683], $P = 1$) exhibits phylogenetic signal; however, total *Wolbachia* at the posterior region had a high, but non-significant λ estimate ($\lambda = 0.907$ [0, 1], $P = 0.423$). The large confidence intervals surrounding these estimates and our simulation analyses **s**uggest total *Wolbachia* fluorescence at the posterior and the pole may exhibit phylogenetic signal, but a larger number of host species ($N = 25, 25$) is required to detect significant departures from $\lambda = 0$ (**Figure 16**). These results suggest that the host genome may also contribute to the diversity of *Wolbachia* localization patterns; however, a larger number of host taxa is required to test this hypothesis.

Table 3. Ectopic growth expression of *Wolbachia* surface proteins in yeast.

Gene	Significant Phylogenetic Signal	Ectopic Expression
WD_1063 (*wsp*/RS04815)	None	Growth inhibition
WD_0009 (*wspB*/RS00060)	None	Growth inhibition
WD_0489 (*wspC*/RS06475)	None	Lethality
WD_1085 (RS04910)	Oocyte posterior, posterior cortex	Growth inhibition and sensitive to microtubule checkpoints/inhibitors
WD_0501 (RS0225)	Oocyte posterior	Slight growth inhibition
WD_1041 (RS04710)	None	Not tested

Figure 15. A) Estimated Bayesian phylogram for host species based on 20 nuclear loci. All nodes have posterior probabilities >0.95. **B)** Mean estimates of *Wolbachia* fluorescence (log-transformed CTCF) in the whole oocyte, posterior region, and the posterior cortex. For *D. simulans*, the mean values include both *w*Ri- and *w*Ha-infected individuals.

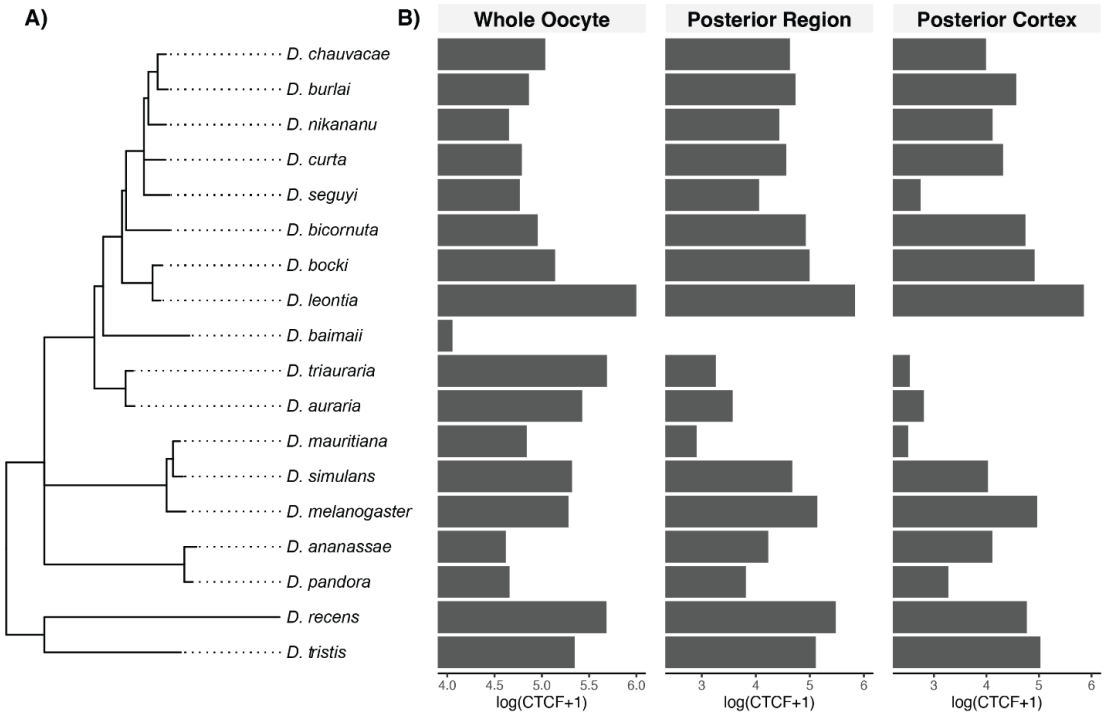

Figure 16. Distribution of maximum likelihood estimates of λ from 1,000 bootstrap replicates based on the host phylogram and *Wolbachia* fluorescence at the oocyte posterior cortex (log-transformed CTCF). The bootstrap analysis of our host phylogram is shown to the left (N = 18 host species). To the right are simulated phylogenies with an increasing number of host species included (N = 25, 50). For simulated trees, character evolution was simulated with our λ estimate of 0.907 using the "sim.bdtree" and "sim.char" functions in the *Geiger* R package (Harmon et al. 2008). For each graph, fitted λ values for the original phylogeny are shown above with a vertical dashed line. Note that fitted λ values for the simulated phylogenies differ slightly from λ = 0.907, because "sim.char" uses a Brownian-motion model to simulate character evolution along the phylogeny. Below each graph, the mean estimate of λ from the 1,000 replicates ($\overline{\lambda}$) is shown with associated 95% confidence intervals. Small phylogenies (e.g., N = 18) are likely to generate many near-zero λ values by chance, not necessarily because the phylogeny is unimportant for trait evolution (Boettiger et al. 2012). As the number of host species in our analysis increases (N = 25, 50), bootstrapped estimates of λ cluster around the true λ value fitted to the original phylogeny.

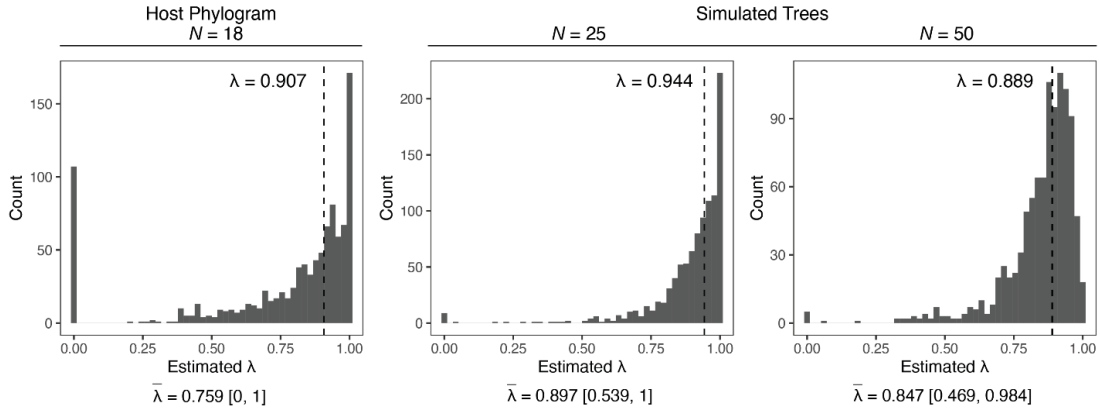

Vertical transmission in some species relies on *Wolbachia* entering the germline from neighboring somatic tissues

Because *Drosophila* species with a dispersed localization have few to no *Wolbachia* at the pole, one would expect that maternal transmission rates may be compromised. However previous studies demonstrated that some of these species, such as *w*Mau-infected *D. mauritiana*, have efficient high maternal transmission rates under standard laboratory conditions (i.e., constant 25ºC) equivalent to that of *w*Mel-infected *D. melanogaster* (Hague et al., 2022; Meany et al., 2019). These findings suggest that in addition to strict germline-to-germline transmission, *Wolbachia* may utilize alternative routes of maternal transmission. Because numerous vertically inherited endosymbionts are transmitted via cell-to-cell transmission from the soma to the germline (Russell *et al.*, 2019), we explored whether *Wolbachia* exploits this strategy.

To determine the developmental stage during which somatic *Wolbachia* invade the germline in this dispersed species, we focused on *w*Mau in *D. mauritiana.* Initially we examined the female germline (oocytes) of 3rd instar larva for the presence of *Wolbachia*. For comparison, we also examined the oocytes of *w*Mel in *D. melanogaster* (a species with a distinct posterior concentration of *Wolbachia*) third instar larval using anti-FtsZ to mark the *Wolbachia* and anti-Vasa to mark the germline. As shown in **Figure 17**, *Wolbachia* is abundantly present in a ring-like patterns in many of the vasa-positive cells in the center of the oocyte. Imaging the oocytes of infected *D. mauritiana* revealed a similar pattern with *Wolbachia* concentrated in the germline stem cells at the center of the oocyte (**Figure 17**).

Figure 17. *Wolbachia*'s presence around the 3rd instar larval germline, in multiple *Drosophila* hosts. *Wolbachia* stained with anti-FtsZ can be seen for *D. mel*, in panel (A) shown in pink. Cells are marked with DAPI (blue). (A') Grayscale channel of anti-FtsZ staining. (B) Uninfected ovary for *D. mel*, (B') grayscale channel for uninfected antibody binding. Germline location marked with anti-vasa shown in green (C), grayscale channel (C'). *Wolbachia* localization in the ovary for *D. Mau* shown in panel (D), grayscale channel (D'). *D. sim* (wRi) shown in panel (E), grayscale (E'). Panel (F), *D. bicornuta*, (F') grayscale channel. Scale bar shown at 25 µM.

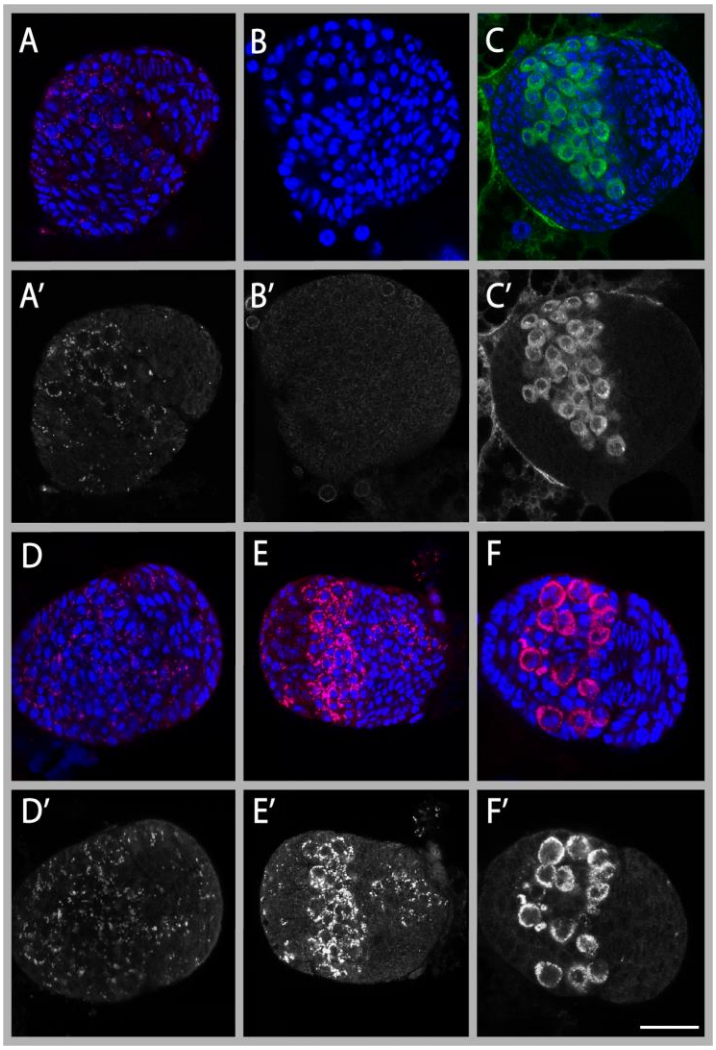

Images of *w*Ri in *D. simulans* as well as *Bicornuta,* species with a dispersed localization and clumped localization in mature oocyte respectively, displayed the same ringlike structure in the oocyte germline of 3rd instar larva, although they appeared to have a much higher titer than *D.mel* or *D.mau* (**Figure 17**). This observation indicates that in species in which vertical transmission occurs with few or no *Wolbachia* present at the site of germline formation in adult oocytes, *Wolbachia* can occupy the germline at some intermediate point. Likely between the final stages of oocyte maturation and development of the fertilized egg into a 3rd instar larva. Presumably the source of the *Wolbachia* is via invasion from neighboring somatic cells.

To determine if *Wolbachia* occupied the germline prior to the 3rd instar larval stage, we examined the newly formed germline of late blastoderm and cellularized embryos. At this stage, newly formed germline cells, known as the pole cells, form a distinct cluster of cells at the extreme posterior to the embryo. In all the four species described above, using PI or anti-*Wolbachia* staining, *Wolbachia* are readily found in these posterior germline cells (**Figure 18)**. Imaging *D. mauritiana* early blastoderm embryos revealed the presence of *Wolbachia* in the posterior pole cells. This observation narrowed the time window at which *Wolbachia* invades and occupies the germlines from between the final stages of oocyte maturation to early blastoderm formation. Images taken of *D. mauritiana* in one-hour embryos also showed *Wolbachia* around the germline narrowing the developmental window of *Wolbachia* germline occupation between the final stages of oocyte maturation to early blastoderm formation (**Figure 18A**)

Figure 18. (A) 1 hour *D. mauritiana* (*w*Mau) embryo stained with PI. (A') Greyscale of PI channel. (B) staining of 2-3 hour developed *D. mauritiana* (*w*Mau) embryo with PI. (B') PI of greyscale channel. (C) PI and anti-vasa (green) staining of *Wolbachia* in 2-3 hour melanogaster embryo. (C') Greyscale of PI channel. (D) anti-FtsZ/DAPI staining for *Wolbachia* in *w*Ri infected *D. simulans*. (D') Greyscale of anti-FtsZ channel. Scale bars set at 25 µM.

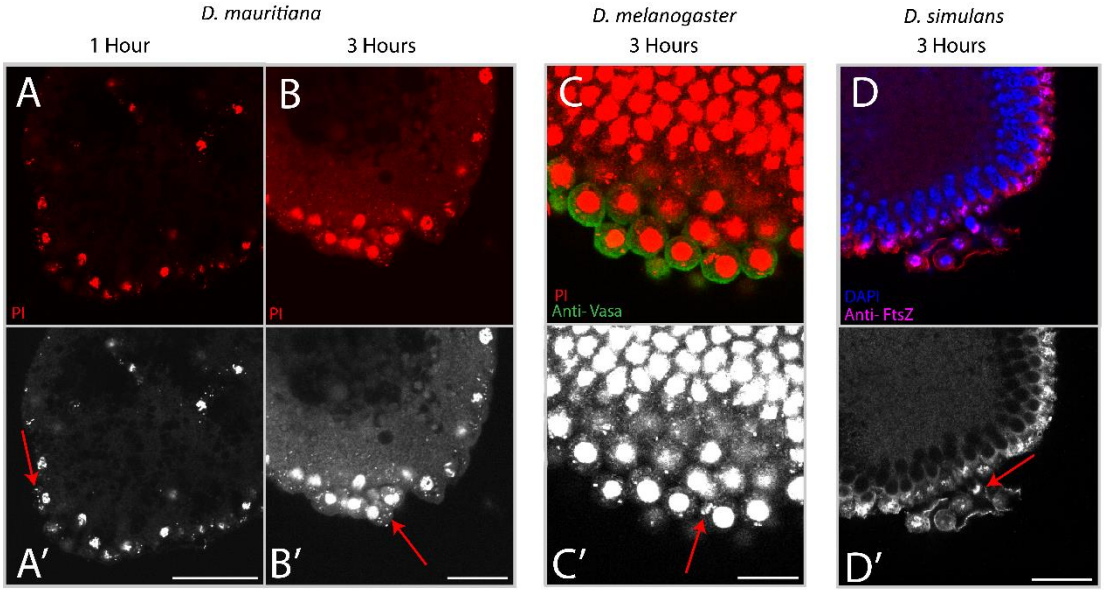

These findings motivated us to examine *D. mauritiana* infected oocytes just prior to egg deposition. Previous studies found that in many infected *Drosophila* species, *Wolbachia* is concentrated in the most posterior positioned follicle cells (Kamath et al., 2018). These somatically derived cells, known as polar cells, directly contact the oocyte posterior pole plasm. In agreeance with previous work (Kamath et al. 2018), we find that while *Wolbachia* are sporadically distributed in subsets of the other follicle cells encompassing the oocyte, its presence in the polar follicle cells is a consistent feature in each of the *D. mauritiana* oocyte examined (**Figure 19K**). These

observations suggest the follicle polar cell *Wolbachia* is the likely somatic source of germline *w*Mau in *D. mauritiana.*

To determine the extent to which *Wolbachia* posterior polar cell localization is a conserved, we analyzed *Wolbachia* localization in the polar and more anterior follicle cells in eight *Drosophila* species with the following patterns: one posteriorly clumped, three posteriorly localized, and four dispersed (**Figure 19**). We scored for the presence of follicle cell *Wolbachia* in each oocyte using the following criteria: Presence in both posterior polar follicle cells, presence in only one polar follicle cell, presence in more anteriorly localized follicle cells. This analysis reveals that in a high percentage of oocytes from dispersed strains (a lack of the *Wolbachia* at the oocyte posterior), *Wolbachia* are presence in the posterior polar follicle cells. In contrast, oocytes examined from strains in which *Wolbachia* are posteriorly concentrated (the posteriorly localized and clumped strains), few possess *Wolbachia* in the posterior follicle cells. Of note, in both *D. Mauritiana* (*w*Mau) and *D. Simulans* (*w*HA + *w*NO), over 78% of their oocytes had both polar cells filled with *Wolbachia*, observationally at higher titer (**Figure 19**). This suggests that in the dispersed species, vertical transmission may be achieved via invasion of *Wolbachia* from the polar follicle cells.

Figure 19 A) Description of *Wolbachia* in the polar follicle cells during stages 9-10 of oogenesis. Midsections of each oocyte were quantified for *Wolbachia* for species that display unique posterior localization patterns, posteriorly clumped, posteriorly located and dispersed B) Description of the number of oocytes observed with *Wolbachia* present anywhere in the follicle cells. (C) Representative anti-FtsZ staining in *D. mauritiana*. Orange labeling corresponds to oocytes having both polar cells infected with *Wolbachia*. (D) Representative staining *in D. melanogaster*. Blue labeling corresponds to oocytes with only one polar cell containing *Wolbachia.* (E) Representative staining of *D. bicornuta.* Grey labeling shows oocytes with no polar cell *Wolbachia*. (F) *D. melanogaster,* with pink labeling describing oocytes where *Wolbachia* was seen anywhere in the follicle cell region. (G-H) Greyscale anti-FtsZ channel of respective composite images above. (K-N) 5X zoom of polar cells, with circles highlighting representative staining in the area. Scale bar set at 25 µM. (O) Schematic of categories used for description of follicle *Wolbachia*. Dispersed posterior localization pattern show, both polar cells infected, with *Wolbachia* broadly present in follicle cells. (P) Posteriorly located species, with one polar cell containing *Wolbachia*, and a distribution of bacteria in the rest of the follicle cell region. (Q) Posteriorly clumped species, with no *Wolbachia* present in the polar cells or greater follicle region.

Figure 19

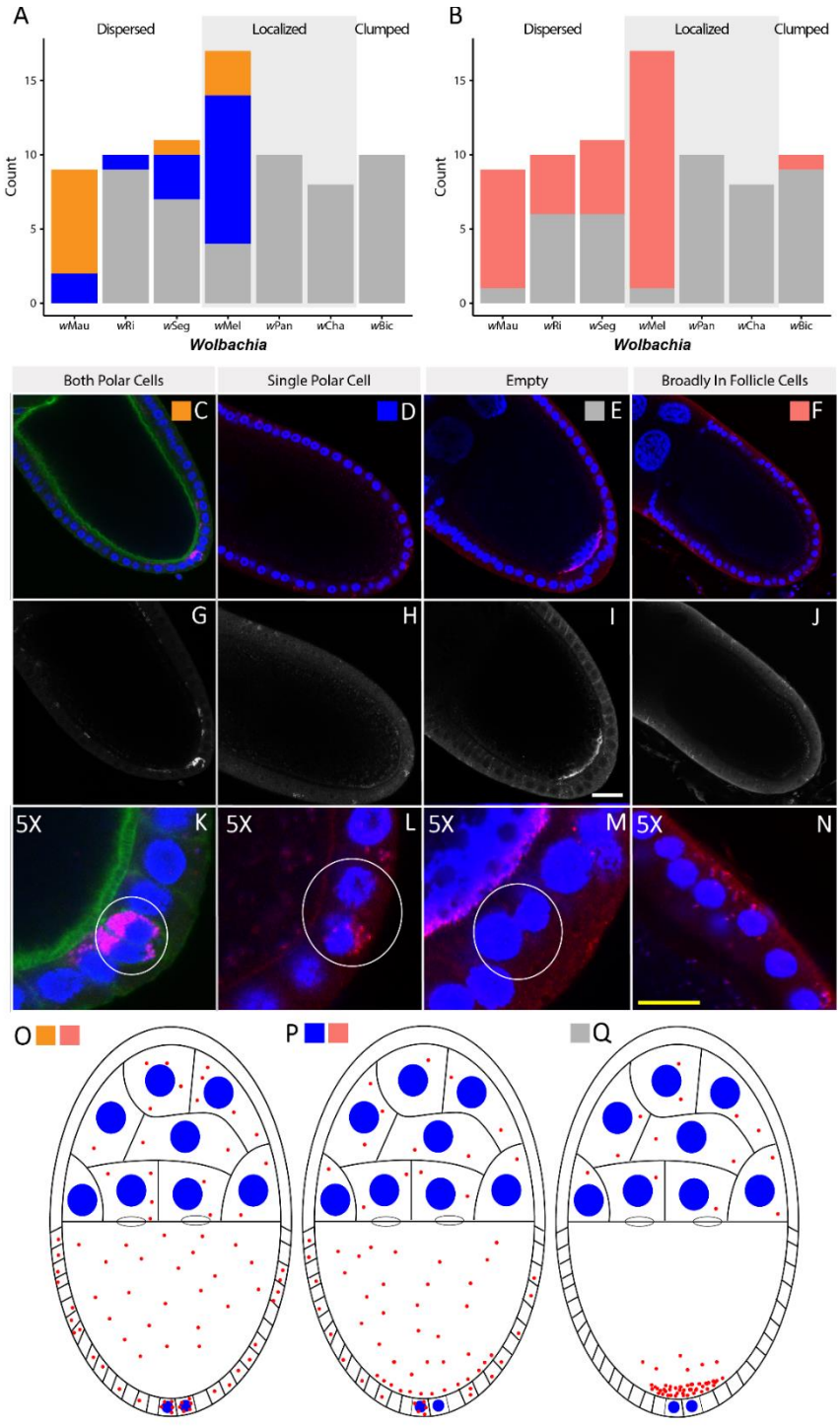
A
Dispersed
Localized
Clumped
Count
wMau
wRi
wSeg
wMel
wPan
wCha
wBic
Wolbachia
B
Dispersed
Localized
Clumped
Count
wMau
wRi
wSeg
wMel
wPan
wCha
wBic
Wolbachia
Both Polar Cells
Single Polar Cell
Empty
Broadly In Follicle Cells
C
D
E
F
G
H
I
J
5X
K
5X
L
5X
M
5X
N
O
P
Q

Material and Methods

Drosophila Stocks

All stocks were grown on standard brown food (Sullivan, 2000) at 25^{o}C with a 12h light/dark cycle. Uninfected *Drosophila* stocks were generated by tetracycline-curing of the infected stock (Serbus *et al.*, 2015). Listed in Table 1 are the 19 different *Wolbachia* strains we examined, which infect 18 different *Drosophila* host species. This included six *w*Mel-like strains (Hague et al., 2020a, Cooper et al., 2019), six *w*Ri-like strains (Turelli *et al.*, 2018), seven other A-group *Wolbachia*, and the B-group strain *w*Mau that diverged from A-group *Wolbachia* up to 36 million years ago (Meany *et al.*, 2019). For each genotype, we imaged the oocytes of an iso-female line generated by sampling a single gravid female from the field and placing her individually into a vial.

Ovary, embryo and larva fixation and staining

Newly eclosed flies were transferred to fresh food for 3-5 days for aging. Approximately 10 females were dissected for each slide preparation. Ovaries were fixed using modification of previously published procedures (Brendza et al., 2000; Russell *et al.*, 2018a). Ovaries were removed and separated in phosphate buffer solution and then fixed in a 200 µl devitellinizing solution (2% paraformaldehyde and 0.5% v/v NP40 in 1x PBS) mixed with 600 µl heptane for 20 min at room temperature, on a shaker. After removal of the organic layer by brief centrifugation for sample isolation, the ovaries were washed 3 times with PBS-T (0.1% Triton X-100 in 1x PBS) along with 3 five-minute washes. Samples were treated with RNase A (10 mg/ml) and left

overnight at room temperature. Samples were then washed three times with PBS-T and then stained with a dilute solution of phalloidin for actin staining on a rotator for 1 hour. Samples were washed again with 3 quick PBS-T rounds and then solution changes with PBS-T over two hours. 60 μL of propidium iodide in mounting media was added to the sample after removal of the wash solution and left again overnight. Ovaries were then mounted and carefully separated out again for ease of imaging and removal of excess mature eggs. Slides were coated in nail polish and stored at -20℃ until imaged.

Embryos were collected for 1-3 hours on plates and fixed in equal volume 32% paraformaldehyde and heptane and fixed as previously described (Sullivan et al., 2000). After extraction with methanol, embryos were blocked for one hour in 5% PBST-BSA (2.5g bovine serum albumin fraction V in 50ml PBS-T) at room temperature. Embryos were then incubated with anti-WD0009 or anti-FtsZ at 1:500 overnight at 4℃. After three washes with 1% PBST-BSA over one hour, embryos were incubated in Alexa 488-anti rabbit at 1:500 for one hour at room temperature. Sample was then washed three more times over one hour with 1% PBST-BSA. Embryos were mounted with media containing DAPI and stored at -20℃ until imaged.

Larval fat bodies were dissected and fixed from third instar larvae using a modified version of a published protocol (Maimon and Gilboa, 2011) and washed in 1X PBS then fixed in 5% paraformaldehyde in PBS for 20 minutes with gentle agitation. Fat bodies were washed for 5 minutes, 10 minutes, then 45 minutes with cold

1% NP40 in PBS. After washes, fat bodies were blocked in 5% PBST-BSA (2.5g bovine serum albumin fraction V in 50ml PBS-T) for one hour at room temperature. Fat bodies were then incubated with anti-FtsZ at 1:500 overnight on a rocker at 4°C, washed three times over one hour with 1% PBST-BSA, then incubated with Alexa 488 Anti-Rabbit at 1:500 at room temperature for one hour. After three additional washes over one hour with 1% PBST-BSA, fat bodies were mounted onto a slide with media containing DAPI. Larval ovaries were isolated from fat bodies using 0.1mm needles before sealing the slide with nail polish. Sample was stored at -20°C.

Confocal microscopy:

Imaging was performed on an inverted Leica DMI6000 SP5 scanning confocal microscope. Optical sections of a Nyquist value of 0.38 were used. A variety of zooms were used to optimize image viewing, with most being set at 1.5X. Propidium iodide was excited with the 514 and 543 nm lasers, and emission from 550 to 680 nm was collected. GFP was imaged with the 488 nm laser, and emission from 488 to 540 nm was collected. Alexa 633 was imaged with the 633 laser, and emission from 606 to 700 nm was collected. All imaging was performed at room temperature. Images were acquired with Leica Application Suite Advanced Fluorescence software.

***Wolbachia* quantification and analysis**

Following Russell et al. (2018), we used the polygon selection tool to select three different regions of the oocyte (see Fig. S1 in Russell et al.): the whole oocyte,

the posterior region, and the posterior cortex. The "area" and "integrated density" were measured for each region. Additionally, the average of a quadruplicate measure of "mean gray value" beside the stained oocytes was measured as background fluorescence. The corrected total cell fluorescence (CTCF) was calculated as integrated density – (area x background mean gray value) for each region. CTCF values were then used to calculate the proportion of total *Wolbachia* fluorescence in the posterior and the pole relative to the whole oocyte.

All statistical analyses were performed in R. We first tested whether our three qualitative classes (clumped, localized, dispersed) differed significantly in quantitative estimates of *Wolbachia* fluorescence (CTCF). We used a one-way ANOVA to test if the three groups differed based on their mean CTCF values from the whole oocyte, the posterior region, and the posterior cortex. Distribution and leverage analyses indicated that a transformation of $x' = \log(x + 1)$ was needed to meet assumptions of normality. We tested for significance using an *F* test with type III sum of squares using the "Anova" function in the *car* package (Fox and Weisberg, 2019) . We conducted post-hoc comparisons among the three groups using the "TukeyHSD" function.

Genomic data

In order to perform the phylogenomic analysis and generate phylograms, we obtained *Wolbachia* sequences from publicly available genome assemblies, which included *w*Mel (Wu et al., 2004), *w*Ri (Klasson et al., 2009), *w*Ha (Ellegaard et al.,

2013), *w*Aura, *w*Tria, *w*Pan (Turelli *et al.*, 2018), *w*Ana (Salzberg et al., 2005), and *w*Rec (Metcalf et al., 2014). All other *Wolbachia* sequences included in this study (*w*Bai, *w*Bic, *w*Boc, *w*Burl, *w*Cha, *w*Curt, *w*Nik, *w*Seg, *w*Tris, *w*Leo) were obtained using Illumina sequencing and previously described methods (Hague *et al.*, 2020b). We obtained publicly available host sequences for *D. melanogaster* (Hoskins et al., 2015), *D. simulans* (Hu et al. 2013), *D. ananassae* (Clark et al., 2007), *D. pandora* (Turelli *et al.*, 2018), *D. mauritiana* (Meany *et al.*, 2019), *D. auraria*, *D. triaurari D. baimaii*, *D. bicornuta*, *D. bocki*, *D. burlai*, *D. chauvacae*, *D. curta*, *D. nikananu*, *D. seguyi*, *D. tristis*, *D. leontia* (Conner, 2021). A *D. recens* genome assembly was kindly provided by Kelly Dyer and Rob Unckless.

Wolbachia phylogenetic analysis

Raw Illumina reads from the newly sequenced *Wolbachia* strains were trimmed using Sickle version 1.33 (Joshi and Fass, 2011) and assembled using ABySS version 2.0.2 (Jackman et al., 2017). *K* values of 71, 81, and 91 were used, and scaffolds with the best nucleotide BLAST matches to known *Wolbachia* sequences with *E*-values less than 10^{-10} were extracted as the draft *Wolbachia* assemblies. For each strain, we chose the assembly with the highest N50 and the fewest scaffolds (**Table 4**). The newly assembled genomes and the previously published assemblies were annotated using Prokka version 1.11, which identifies homologs to known bacterial genes (Seemann, 2014). To avoid pseudogenes and paralogs, we only used genes present in a single copy with no alignment gaps in all the genome sequences. Genes were identified as single

copy if they uniquely matched a bacterial reference gene identified by Prokka. By requiring all homologs to have identical length in all the *Wolbachia* genomes, we removed all loci with indels. A total of 66 genes totaling 43,275 bp met these criteria. We then estimated a Bayesian phylogram using RevBayes 1.0.8 under the GTR + Γ + I model partitioned by codon position (Höhna et al., 2016). Four independent runs were performed, which all converged on the same topology. All nodes were supported with Bayesian posterior probabilities of 1.

Table 4. Scaffold count, N50, and total assembly size of each new *Wolbachia* assembly.

Host species	*Wolbachia*	Scaffold Count	N50	Total Assembly Size
D. baimaii	*w*Bia	209	9004	1135209
D. bicornuta	*w*Bic	140	16267	1192611
D. bocki	*w*Boc	227	7115	1090928
D. burlai	*w*Burl	128	20905	1248003
D. chauvacae	*w*Cha	406	4802	1300201
D. curta	*w*Curt	59	29597	1132109
D. nikananu	*w*Nik	83	22663	1257108
D. seguyi	*w*Seg	201	8880	1174927
D. tristis	*w*Tris	114	20171	1264866
D. leontia	*w*Leo	186	9149	1096851

Similar methods were used to generate gene trees for candidate *Wolbachia* loci putatively involved in host interactions during oogenesis. This included the three *wsp* paralogs (WD1063, WD0009, WD0489) and three other *Wolbachia* surface proteins (WD1085, WD0501, WD1041). The protein-coding sequences for each locus were extracted from the assemblies using BLAST and the *w*Mel reference sequences. Notably, we found evidence of insertions in the *wspB* sequences of *w*Boc, *w*Leo, and

*w*Bic (see Results). We removed these large insertions from the alignment to generate the *wspB* gene tree. In addition, BLAST identified *wspC* (WD0489) in *w*Mel-like *Wolbachia* and closely related *w*Bai, *w*Leo, and *w*Bok, but yielded no hits in the other *Wolbachia* strains (*w*Nik, *w*Curt, *w*Pan, *w*Ana, *w*Tria, *w*Aura, *w*Ri, *w*Mau), indicating that *wspC* is too diverged from the *w*Mel reference for BLAST recognition or alternatively *wspC* is only present in *w*Mel-related *Wolbachia* strains. Sequences for each gene were aligned with MAFFT 7 (Katoh and Standley, 2013). We then used RevBayes and the GTR + Γ + I model partitioned by codon position to generate gene trees for each locus.

Host phylogenetic analysis

Host phylogenies were generated using the same nuclear genes implemented in Turelli et al. (2018): *aconitase, aldolase, bicoid, ebony, enolase, esc, g6pdh, glyp, glys, ninaE, pepck, pgi, pgm, pic, ptc, tpi, transaldolase, white, wingless,* and *yellow*. We used BLAST with the *D. melanogaster* coding sequences to extract orthologs from the genomes of each host species. Sequences were then aligned with MAFFT 7. Finally, we used RevBayes and the GTR + Γ + I model partitioned by codon position and gene to accommodate potential variation in the substitution process among genes, as described in Turelli et al. (2018).

Tests for phylogenetic signal

The resulting phylograms were used to test whether cellular *Wolbachia*

abundance in oocytes exhibits phylogenetic signal on either the *Wolbachia* or host phylogenies. We used our quantitative estimates of *Wolbachia* abundance to test for phylogenetic signal using Pagel's lambda (λ) (Pagel, 1999). Here, we used total *Wolbachia* fluorescence in whole oocytes, the posterior region, and the posterior cortex (log-transformed CTCF) as continuous characters to calculate maximum likelihood values of Pagel's. A Pagel's λ of 0 indicates that character evolution occurs independently of phylogenetic relationships, whereas λ = 1 is consistent with a Brownian motion model of character evolution. We used the "fitContinuous" function in GEIGER (Harmon et al., 2008) and a likelihood ratio test to compare our fitted value of to a model assuming no phylogenetic signal (λ = 0). We also used a Monte Carlo-based method to generate 95% confidence intervals surrounding our estimate using 1,000 bootstrap replicates in the *pmc* package (Boettiger et al., 2012). When applicable, we conducted additional analyses to evaluate whether the number of taxa in our phylogeny (*N* = 19 *Wolbachia* strains, *N* = 18 host species) limited our ability to detect significant departures from λ = 0 (Hague *et al.*, 2020b; Hague *et al.*, 2021). Small phylogenies are likely to generate near-zero values simply by chance, not necessarily because the phylogeny is unimportant for trait evolution (Boettiger *et al.*, 2012). To evaluate whether larger phylogenies increase the accuracy of estimation, we simulated trees with an increasing number of *Wolbachia* strains/host species (*N* = 25, 50) and our empirical estimates using the "sim.bdtree" and "sim.char" functions in the *geiger* R package (Harmon *et al.*, 2008). We then re-estimated confidence intervals, using the larger simulated trees

Discussion

Vertical transmission through the female lineage is a common strategy for many endosymbionts. Prior analysis revealed these endosymbionts achieve high efficiencies of maternal transmission either through direct germline-to-germline transmission or invasion of the maternal germline through neighboring somatic cells (Russell *et al.*, 2019). Because the former involves a continuous presence in the germline while the latter requires navigating a, soma-to-germline passage, it is expected that each requires distinct interactions with and manipulations of host cellular processes. Thus, it would be expected that a given endosymbiont would have evolved to utilize one, but not both of these strategies. Here we explore this issue by examining the cellular aspects of *Wolbachia* vertical transmission that are conserved and those that vary. In contrast to expectations, by carrying out the most comprehensive analysis of the cell biology of endosymbiont transmission to date, we find that across 19 diverse systems, *Wolbachia* relies on both strict germline-to-germline and soma-to-germline vertical transmission strategies.

The cellular aspects of *w*Mel *Wolbachia* transmission have been well characterized in *D. melanogaster* (Serbus *et al.*, 2008). During early oogenesis, *Wolbachia* relies on microtubules and the minus end motor protein dynein for transport from the 15 nurse cells to the newly formed oocyte (all connected through cytoplasmic bridges) (Ferree *et al.*, 2005). *Wolbachia* enter and accumulate at the anterior end of the oocyte. At this point in oogenesis, the microtubules undergo a dramatic

reorganization such that they orient with their plus-ends directed toward the posterior pole. Concomitant with this reversal of polarity, the *Wolbachia* are released from the anterior cortex and are distributed throughout the entire oocyte with a subset concentrating at the posterior pole. Concentration and maintenance at the posterior pole require kinesin and an intact pole plasm, respectively (Russell *et al.*, 2018b; Serbus and Sullivan, 2007).

The initial anterior localization of *Wolbachia* in the developing oocyte, appears to be a conserved aspect of *Wolbachia* transmission, as all eight species examined exhibit a distinct anterior localization. It is striking that this localization occurs prior to any known anterior determinant, indicating *Wolbachia* may associate with an as yet undiscovered host factor concentrated at the anterior. That this localization is conserved suggests that it may have a functionally significant, but currently unknown role in *Wolbachia* transmission. While anteriorly localized, the amount of *Wolbachia* dramatically increases. Whether *Wolbachia* replication, transport from the nurse cells, or both are responsible for this increase is unknown. The anterior location may be a rich source of membrane for *Wolbachia* replication. The anterior localization also results in a high concentration of *Wolbachia* that closely associated with, and perhaps influences, the oocyte nucleus.

To our surprise, we discovered that just after the release of *Wolbachia* from its anterior position in the oocyte (Stage 6), the amount of *Wolbachia* oocyte dramatically decreases (see Figure 1 stage 6 and Figure 2). This suggests that the *Wolbachia* may be

transported back into the nurse cell complex, or alternatively be degraded by the host. The functional significance of this clearing of *Wolbachia* from the oocyte is unknown, as well as the exact mechanism occurring. The retreat of *Wolbachia* occurs during the time when the anterior positioned oocyte and neighboring follicle cells signal one another to establish the dorsal ventral axis (Merkle et al., 2020). Perhaps *Wolbachia* exits the oocyte to avoid disrupting this process. Given the orientation of microtubules at this stage, it is likely *Wolbachia* rapidly exits the oocyte through an association with the plus-end directed motor kinesin.

Following microtubule reorientation and the return of *Wolbachia* to the oocyte, *Wolbachia* spreads posteriorly throughout the entire oocyte relying on the host motor protein kinesin (Serbus and Sullivan, 2007). All of the *Wolbachia* strains examined are distributed toward the posterior regions suggesting the interaction with kinesin is also conserved. How *Wolbachia* engages these motor proteins is unknown. Surprisingly none of the known host kinesin linker proteins are utilized by *Wolbachia*, suggesting *Wolbachia* may interact directly with kinesin (Russell *et al.*, 2018b).

It is immediately after this stage in which *Wolbachia* are distributed throughout the oocyte, that we observe variability in the 18 *Wolbachia*-infected species with each falling into one of three distinct classes: two distinct classes in which *Wolbachia* concentrate at the posterior (posteriorly localized and posteriorly clumped) and one class in which *Wolbachia* fail to exhibit a posterior concentration (Dispersed). The former two classes are distinguished by whether the vast majority (posteriorly-

clumped) or only a small fraction of the *Wolbachia* localize to the posterior pole (Posteriorly localized).

The posteriorly localized class in which only a small fraction localize to the posterior pole can be explained by previous work demonstrating that *w*Mel is a weak competitor for kinesin both *Wolbachia* and germplasm components rely on kinesin for transport to the posterior pole (Russell *et al.*, 2018b). To ensure that *Wolbachia* does not interfere with the transport of essential germplasm components and thus germplasm formation, it is thought that *Wolbachia* has evolved to be a weak competitor. The other posterior class (posteriorly clumped) is strikingly similar to that observed in *D. melanogaster* in which the plus end motor protein kinesin is over-expressed and excess amounts of *Wolbachia* are transported to the posterior pole (Russell *et al.*, 2018b). It may be that in the posteriorly-clumped infected species there are naturally much higher levels of host kinesin or that the specific *Wolbachia* is a much better competitor for host kinesin. It would be interesting to investigate whether there are instances in which *Wolbachia* disrupts the A-P axis (anterior-posterior) because of its accumulation at the posterior pole.

The variability in posterior pole concentration among *Wolbachia* strains also may be due to variability in the ability of *Wolbachia* to stably associate with the pole plasm. Previous studies demonstrated that *Wolbachia* posterior pole concentration requires intact pole plasm (Serbus and Sullivan, 2007). For example, in *oskar* mutations, a key pole plasm determinant, *w*Mel-*Wolbachia* fails to accumulate at the

posterior region. As described the oocyte experiences tremendous cytoplasmic streaming requiring posterior components to be anchored directly or indirectly to the cortex (Quinlan, 2016). This variability could be due to differences in the ability of *Wolbachia* to compete with other pole plasm components such as mitochondria for binding sites. Alternatively, the host species may vary in the extent to which their pole plasm accommodates *Wolbachia*. These alternatives can be explored through trans-infection studies.

The overlapping, but distinct, *Wolbachia* oocyte localization patterns suggest corresponding intertwined interactions with host factors among the three *Wolbachia* classes of posterior localization. This variation in the host proteins with which *Wolbachia* engages contrasts with other endosymbionts such as *Listeria*. *Listeria* relies on a surface protein, which binds and polymerizes host actin, propelling it both within and between host cells (Kühn and Enninga, 2020). Because the interaction between ActA and actin is essential for cell-to-cell transmission, natural variants of this interaction and transmission strategy have not been discovered. Thus, the variation in *Wolbachia* oocyte localization suggests variation in the host proteins in which multiple strategies of vertical transmission are possible.

Two classes in which *Wolbachia* concentrates in the posterior pole (posteriorly localized and posteriorly clumped) provide a ready explanation for the cellular mechanisms by which it is vertically transmitted through generations. In every generation, *Wolbachia* targets the site of germline formation in the developing oocyte.

This also explains why strains exhibiting this pattern, such as *w*Mel, exhibit efficient transmission strategies under typical laboratory conditions (Hague et al., 2022). The third, Distributed, class that exhibits no-to-low *Wolbachia* in the posterior germplasm of the mature oocyte is puzzling. This would be expected to result in embryos lacking *Wolbachia* in the germline. However, within hours after fertilization, *Wolbachia* is clearly present in the germlines of both sexes (**Figure 6**). This implies that in these strains *Wolbachia* can invade the germline from neighboring somatic cells. In filarial nematodes, *Wolbachia* germline invasion from the soma has been directly observed (Landmann et al., 2012). While germline invasion via cell-to-cell transmission has not been directly observed in insects, several lines of evidence indicate that it likely occurs. In *Drosophila* cell culture, *Wolbachia* efficiently undergoes cell-to-cell transmission (White et al., 2017; White et al., 2017). *Wolbachia* injected into the abdomen of adult *Drosophila* females migrate to and occupy the germline and follicle stem cells (Frydman et al., 2006). Collections directly from nature reveal some strains with developing oocytes lacking Wolbachia (Casper-Lindley et al., 2011). In these strains, all the mature oocytes were infected, suggesting an alternate route of infection via neighboring somatic cells.

Given the posterior follicle cells are directly adjacent to the pole plasm, we suspect *Wolbachia* present in the latter are the source of germline *Wolbachia*. As found in female filarial nematodes, this requires that *Wolbachia* undergo cell-to-cell transmission (Landmann *et al.*, 2012). Our results are in accord with and complement previous studies demonstrating *Wolbachia* concentrated in the posterior polar follicle

cells in a number of *Wolbachia*-infected species (Kamath *et al.*, 2018). For example, in *w*Mau-infected *D. mauritiana*, a dispersed class, there is a striking concentration of *Wolbachia* in the posterior follicle pole cells directly adjacent to the pole plasm. Thus, *Wolbachia* in these somatic cells are well positioned to invade the pole plasm becoming incorporated into the germline of the next generation (**Figure 20**). In contrast, in the posteriorly localized and clumped strains, none to few *Wolbachia* are present in the posterior polar follicle cells. As *Wolbachia* are germline-to-germline transmitted in these strains, there is no need for a presence in the polar follicle cells. Among the *Wolbachia* strains examined, *w*Mel stands out as an exception. Not only is it concentrated at the posterior pole of the oocyte, but also a large concentration of *Wolbachia* are present in the posterior polar follicle cells. Thus, *w*Mel may maintain both robust germline-to-germline and soma-to-germline modes of transmission. Accordingly, it has an extremely high efficiency of vertical transmission. Surprisingly surveys of the literature reveal invasion of the germline from the soma every generation is the most common form of vertical inheritance (Russell *et al.*, 2019). Vertical transmission via a continuous presence in the germline is much less common. One explanation is that host maintains mechanisms preventing endosymbiont occupation during the formative stages of germline development. In instances in which the endosymbiont is maintained in the germline, this may evolve into an obligate relationship in which development of the germline depends on the presence of the endosymbiont (Sullivan, 2017). Examples of this include the leafhopper (*E. plebeus*), in which the endosymbiont is required for normal embryonic development (Sander,

1968). In addition, removal of *Wolbachia* from some insects results in increased apoptosis and abnormal oocyte development (Dedeine et al., 2001; Pannebakker et al., 2007).

Examining a diversity of *Wolbachia* strains and host species enabled us to test whether *Wolbachia* oocyte abundance and localization are correlated with the evolutionary relationships of the *Wolbachia* strains or host species. This analysis revealed a strong correlation between *Wolbachia* posterior abundance and *Wolbachia* phylogenetic relationships, suggesting that factors intrinsic to *Wolbachia* contribute to posterior localization patterns. Generally, we find that closely related *w*Mel-like *Wolbachia* occur at higher abundance at the oocyte posterior, whereas *w*Ri-like *Wolbachia* exhibit a more dispersed distribution (**Figure 9**). This conclusion in accord with previous *Wolbachia* transplantation studies demonstrating that posterior localization is determined by *Wolbachia* rather than host factors (Veneti *et al.*, 2004) (Serbus and Sullivan, 2007). It is likely that the composition of *Wolbachia* surface proteins play a major role in the extent of posterior localization.

Figure 20. Routes of germline invasion. (A) In strains with posteriorly localized *Wolbachia* positioning, a presence at the pole plasm ensures germline to germline transfer between generations. (B) *Wolbachia* which display a dispersed localization pattern likely use a soma to germline method. Given the high titer of *Wolbachia* in the pole cells, this model presents during stages 10B-14 of oogenesis they invade into the oocyte region and now maintain the same posterior localization around the developing germline as those with an early oocyte posterior localization. (C) Hypothetical soma to soma transmission. Circles show possible movement of *Wolbachia* from the soma to germline as the cycle repeats in the next generation. While not shown in the data collected for this work, it is likely important for initial infection of the germline when invading a new species or an uninfected fly.

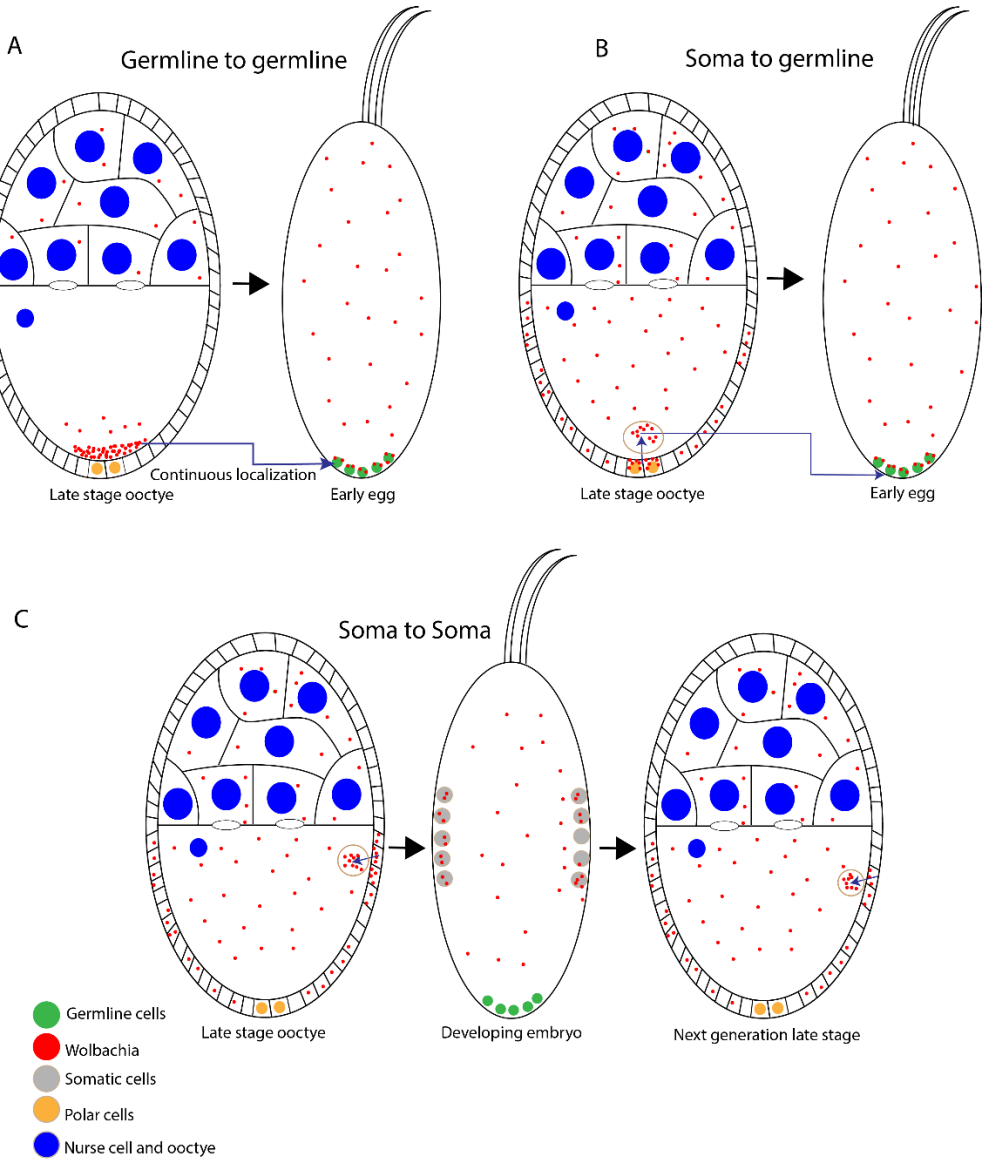

We did not find that *Wolbachia* localization patterns exhibit significant phylogenetic signal on the host phylogeny; however, our simulations suggest this may be due to limited power (**Figure 11**) such that host-associated factors could contribute to *Wolbachia* localization patterns. This result is also in accord with the transplantation studies described above revealing that hosts also plays a significant role in determining *Wolbachia* abundance (Veneti *et al.*, 2004). In addition, genome-wide screens reveal host factors play a major role in determining *Wolbachia* intracellular abundance (Grobler et al., 2018)(White et al., 2017b). Finally, nutrients and other environmental factors influence *Wolbachia* abundance in the oocyte and maternal transmission rates for closely related wMel-like *Wolbachia* (Hague *et al.*, 2020b; Hague *et al.*, 2022; Serbus et al., 2015).

To identify specific *Wolbachia* factors promoting posterior localization, we performed the same phylogenetic analysis using gene trees of the six predicted *Wolbachia* surface proteins. This analysis revealed that two candidate surface proteins, particularly WD1085, exhibited strong phylogenetic signal associated with *Wolbachia* localization patterns. While we highlight these loci as potential candidates, we note that our results should be interpreted with caution because the entire genomes of vertically transmitted endosymbionts like *Wolbachia* are in strong linkage disequilibrium, making it difficult to attribute causation to any specific locus. For example, the surface protein WD1085 could be in strong linkage with causal loci. Nonetheless, *Wolbachia* surface proteins are generally considered to be strong candidates for interactions with host cells (Baldridge et al., 2016; Hague *et al.*, 2022; Werren et al., 2008).

This work provides several insights into the diversity and non-intuitive nature of *Wolbachia* localization during oogenesis, as well as proteins whose role is yet to be fully elucidated. While this analysis furthers the hypothesis of soma to germline transmission in *drosophila*, additional exploration will be needed to determine the exact stage of invasion and how this process might vary between *Wolbachia* strains.

Bibliography

Baldridge, G.D., Li, Y.G., Witthuhn, B.A., Higgins, L., Markowski, T.W., Baldridge, A.S., and Fallon, A.M. (2016). Mosaic composition of *ribA* and *wspB* genes flanking the virB8-D4 operon in the *Wolbachia* supergroup B-strain, *w*Str. Arch Microbiol *198*, 53-69. 10.1007/s00203-015-1154-8.

Bastock, R., and St Johnston, D. (2008). *Drosophila* oogenesis. Curr Biol *18*, R1082-1087. 10.1016/j.cub.2008.09.011.

Bilinski, S.M., Jaglarz, M.K., and Tworzydlo, W. (2017). The Pole (Germ) Plasm in Insect Oocytes. Results Probl Cell Differ *63*, 103-126. 10.1007/978-3-319-60855-6_5.

Boettiger, C., Coop, G., and Ralph, P. (2012). Is your phylogeny informative? Measuring the power of comparative methods. Evolution *66*, 2240-2251. 10.1111/j.1558-5646.2011.01574.x.

Brendza, R.P., Serbus, L.R., Duffy, J.B., and Saxton, W.M. (2000). A function for kinesin I in the posterior transport of oskar mRNA and Staufen protein. Science *289*, 2120-2122. 10.1126/science.289.5487.2120.

Carrington, L.B., Lipkowitz, J.R., Hoffmann, A.A., and Turelli, M. (2011). A re-examination of *Wolbachia*-induced cytoplasmic incompatibility in California *Drosophila* simulans. PLoS One *6*, e22565. 10.1371/journal.pone.0022565.

Casper-Lindley, C., Kimura, S., Saxton, D.S., Essaw, Y., Simpson, I., Tan, V., and Sullivan, W. (2011). Rapid fluorescence-based screening for *Wolbachia* endosymbionts in *Drosophila* germ line and somatic tissues. Appl Environ Microbiol *77*, 4788-4794. 10.1128/AEM.00215-11.

Cha, B.J., Koppetsch, B.S., and Theurkauf, W.E. (2001). In vivo analysis of *Drosophila bicoid* mRNA localization reveals a novel microtubule-dependent axis specification pathway. Cell *106*, 35-46. 10.1016/s0092-8674(01)00419-6.

Cha, B.J., Serbus, L.R., Koppetsch, B.S., and Theurkauf, W.E. (2002). Kinesin I-dependent cortical exclusion restricts pole plasm to the oocyte posterior. Nat Cell Biol *4*, 592-598. 10.1038/ncb832.

Clark, A.G., Eisen, M.B., Smith, D.R., Bergman, C.M., Oliver, B., Markow, T.A., Kaufman, T.C., Kellis, M., Gelbart, W., Iyer, V.N., et al. (2007). Evolution of genes and genomes on the *Drosophila* phylogeny. Nature *450*, 203-218. 10.1038/nature06341.

Cogni, R., Ding, S.D., Pimentel, A.C., Day, J.P., and Jiggins, F.M. (2021). *Wolbachia* reduces virus infection in a natural population of *Drosophila*. Commun Biol *4*, 1327. 10.1038/s42003-021-02838-z.

Conner, W. (2021). A phylogeny for the *Drosophila* montium species group: A model clade for comparative analyses. Molecular Phylogenetics and Evolution *158*, 107061.

Conner, W.R., Blaxter, M.L., Anfora, G., Ometto, L., Rota-Stabelli, O., and Turelli, M. (2017). Genome comparisons indicate recent transfer of. Ecol Evol *7*, 9391-9404. 10.1002/ece3.3449

Cooper, B.S., Ginsberg, P.S., Turelli, M., and Matute, D.R. (2017). *Wolbachia* in the *Drosophila* yakuba Complex: Pervasive Frequency Variation and Weak Cytoplasmic Incompatibility, but No Apparent Effect on Reproductive Isolation. Genetics *205*, 333-351. 10.1534/genetics.116.196238.

Cooper, B.S., Vanderpool, D., Conner, W.R., Matute, D.R., and Turelli, M. (2019). Acquisition by. Genetics *212*, 1399-1419. 10.1534/genetics.119.302349.

Cooper BS, Vanderpool D, Conner WR, Matute DR, Turelli M. 2019. *Wolbachia* acquisition by *Drosophila* yakuba-clade hosts and transfer of incompatibility loci between distantly related *Wolbachia*. Genetics 212: 1399 –1419)

Cummings, M.R., Brown, N.M., and King, R.C. (1971). The cytology of the vitellogenic stages of oogenesis in *Drosophila* melanogaster. 3. Formation of the vitelline membrane. Z Zellforsch Mikrosk Anat *118*, 482-492. 10.1007/BF00324615.

Dedeine, F., Vavre, F., Fleury, F., Loppin, B., Hochberg, M.E., and Bouletreau, M. (2001). Removing symbiotic *Wolbachia* bacteria specifically inhibits oogenesis in a parasitic wasp. Proc Natl Acad Sci U S A *98*, 6247-6252. 10.1073/pnas.101304298.

Ellegaard, K.M., Klasson, L., Näslund, K., Bourtzis, K., and Andersson, S.G. (2013). Comparative genomics of *Wolbachia* and the bacterial species concept. PLoS Genet *9*, e1003381. 10.1371/journal.pgen.1003381.

Ferree, P.M., Frydman, H.M., Li, J.M., Cao, J., Wieschaus, E., and Sullivan, W. (2005). *Wolbachia* utilizes host microtubules and Dynein for anterior localization in the *Drosophila* oocyte. PLoS Pathog *1*, e14. 10.1371/journal.ppat.0010014.

Fox, J., and Weisberg, S. (2019). An R companion to applied regression. SAGE.

Freckleton, R.P., Harvey, P.H., and Pagel, M. (2002). Phylogenetic analysis and comparative data: a test and review of evidence. Am Nat *160*, 712-726. 10.1086/343873.

Frydman, H.M., Li, J.M., Robson, D.N., and Wieschaus, E. (2006). Somatic stem cell niche tropism in *Wolbachia*. Nature *441*, 509-512. 10.1038/nature04756.

Gerth, M., and Bleidorn, C. (2016). Comparative genomics provides a timeframe for *Wolbachia* evolution and exposes a recent biotin synthesis operon transfer. Nat Microbiol *2*, 16241. 10.1038/nmicrobiol.2016.241.

Grieder, N.C., de Cuevas, M., and Spradling, A.C. (2000). The fusome organizes the microtubule network during oocyte differentiation in *Drosophila*. Development *127*, 4253-4264.

Guo, Y., Gong, J.T., Mo, P.W., Huang, H.J., and Hong, X.Y. (2019). *Wolbachia* localization during Laodelphax striatellus embryogenesis. J Insect Physiol *116*, 125-133. 10.1016/j.jinsphys.2019.05.006.

Hague, M.T.J., Caldwell, C.N., and Cooper, B.S. (2020b). Pervasive Effects of *Wolbachia* on host temperature preference. mBio *11*. 10.1128/mBio.01768-20.

Hague, M.T.J., Mavengere, H., Matute, D.R., and Cooper, B.S. (2020a). Environmental and Genetic Contributions to Imperfect wMel-like *Wolbachia* Transmission and Frequencies. Genetics *215*, 1117-1132. 10.1534/genetics.120.303330.

Hague, M.T.J., Shropshire, J.D., Caldwell, C.N., Statz, J.P., Stanek, K.A., Conner, W.R., and Cooper, B.S. (2021). Temperature effects on cellular host-microbe interactions explain continent-wide endosymbiont prevalence. Curr Biol. 10.1016/j.cub.2021.11.065.

Hague, M.T.J., Shropshire, J.D., Caldwell, C.N., Statz, J.P., Stanek, K.A., Conner, W.R., and Cooper, B.S. (2022). Temperature effects on cellular host-microbe interactions explain continent-wide endosymbiont prevalence. Curr Biol *32*, 878-888.e878. 10.1016/j.cub.2021.11.065.

Harmon, L.J., Weir, J.T., Brock, C.D., Glor, R.E., and Challenger, W. (2008). GEIGER: investigating evolutionary radiations. Bioinformatics *24*, 129-131. 10.1093/bioinformatics/btm538.

Hoffmann, A.A., Hercus, M., and Dagher, H. (1998). Population dynamics of the *Wolbachia* infection causing cytoplasmic incompatibility in *Drosophila* melanogaster. Genetics *148*, 221-231. 10.1093/genetics/148.1.221.

Hoffmann, A.A., Turelli, M., and Harshman, L.G. (1990). Factors affecting the distribution of cytoplasmic incompatibility in *Drosophila* simulans. Genetics *126*, 933-948. 10.1093/genetics/126.4.933.

Höhna, S., Landis, M.J., Heath, T.A., Boussau, B., Lartillot, N., Moore, B.R., Huelsenbeck, J.P., and Ronquist, F. (2016). RevBayes: Bayesian Phylogenetic Inference Using Graphical Models and an Interactive Model-Specification Language. Syst Biol *65*, 726-736. 10.1093/sysbio/syw021.

Hoskins, R.A., Carlson, J.W., Wan, K.H., Park, S., Mendez, I., Galle, S.E., Booth, B.W., Pfeiffer, B.D., George, R.A., Svirskas, R., et al. (2015). The Release 6 reference sequence of the *Drosophila* melanogaster genome. Genome Res *25*, 445-458. 10.1101/gr.185579.114.

Jackman, S.D., Vandervalk, B.P., Mohamadi, H., Chu, J., Yeo, S., Hammond, S.A., Jahesh, G., Khan, H., Coombe, L., Warren, R.L., and Birol, I. (2017). ABySS 2.0: resource-efficient assembly of large genomes using a Bloom filter. Genome Res *27*, 768-777. 10.1101/gr.214346.116.

Joshi, N., and Fass, J. (2011). Sickle: a sliding-window, adaptive, quality-based trimming tool for FastQ files.

Katoh, K., and Standley, D.M. (2013). MAFFT multiple sequence alignment software version 7: improvements in performance and usability. Mol Biol Evol *30*, 772-780. 10.1093/molbev/mst010.

Klasson, L., Westberg, J., Sapountzis, P., Näslund, K., Lutnaes, Y., Darby, A.C., Veneti, Z., Chen, L., Braig, H.R., Garrett, R., et al. (2009). The mosaic genome structure of the *Wolbachia* wRi strain infecting *Drosophila* simulans. Proc Natl Acad Sci U S A *106*, 5725-5730. 10.1073/pnas.0810753106.

Kose, H., and Karr, T.L. (1995). Organization of *Wolbachia* pipientis in the *Drosophila* fertilized egg and embryo revealed by an anti-*Wolbachia* monoclonal antibody. Mech Dev *51*, 275-288. 10.1016/0925-4773(95)00372-x.

Kühn, S., and Enninga, J. (2020). The actin comet guides the way: How *Listeria* actin subversion has impacted cell biology, infection biology and structural biology. Cell Microbiol *22*, e13190. 10.1111/cmi.13190.

Mahajan-Miklos, S., and Cooley, L. (1994). Intercellular cytoplasm transport during *Drosophila* oogenesis. Dev Biol *165*, 336-351. 10.1006/dbio.1994.1257.

Mahowald, A.P., and Strassheim, J.M. (1970). Intercellular migration of centrioles in the germarium of *Drosophila* melanogaster. An electron microscopic study. J Cell Biol *45*, 306-320. 10.1083/jcb.45.2.306.

Maimon, I., and Gilboa, L. (2011). Dissection and staining of *Drosophila* larval ovaries. J Vis Exp. 10.3791/2537.

Meany, M.K., Conner, W.R., Richter, S.V., Bailey, J.A., Turelli, M., and Cooper, B.S. (2019). Loss of cytoplasmic incompatibility and minimal fecundity effects explain relatively low *Wolbachia* frequencies in *Drosophila* mauritiana. Evolution *73*, 1278-1295. 10.1111/evo.13745.

Merkle, J.A., Wittes, J., and Schüpbach, T. (2020). Signaling between somatic follicle cells and the germline patterns the egg and embryo of *Drosophila*. Curr Top Dev Biol *140*, 55-86. 10.1016/bs.ctdb.2019.10.004.

Metcalf, J.A., Jo, M., Bordenstein, S.R., and Jaenike, J. (2014). Recent genome reduction of *Wolbachia* in *Drosophila* recens targets phage WO and narrows candidates for reproductive parasitism. PeerJ *2*, e529. 10.7717/peerj.529.

O'Neill, S.L., Giordano, R., Colbert, A.M., Karr, T.L., and Robertson, H.M. (1992). 16S rRNA phylogenetic analysis of the bacterial endosymbionts associated with cytoplasmic incompatibility in insects. Proc Natl Acad Sci U S A *89*, 2699-2702. 10.1073/pnas.89.7.2699.

Pagel, M. (1999). Inferring the historical patterns of biological evolution. Nature *401*, 877-884. 10.1038/44766.

Pannebakker, B.A., Loppin, B., Elemans, C.P., Humblot, L., and Vavre, F. (2007). Parasitic inhibition of cell death facilitates symbiosis. Proc Natl Acad Sci U S A *104*, 213-215. 10.1073/pnas.0607845104.

Ramalho, M.O., Vieira, A.S., Pereira, M.C., Moreau, C.S., and Bueno, O.C. (2018). Transovarian Transmission of Blochmannia and *Wolbachia* Endosymbionts in the Neotropical Weaver Ant Camponotus textor (Hymenoptera, Formicidae). Curr Microbiol *75*, 866-873. 10.1007/s00284-018-1459-3.

Raychoudhury, R., Baldo, L., Oliveira, D.C., and Werren, J.H. (2009). Modes of acquisition of *Wolbachia*: horizontal transfer, hybrid introgression, and codivergence in the *Nasonia* species complex. Evolution *63*, 165-183. 10.1111/j.1558-5646.2008.00533.x.

Russell, S.L., Chappell, L., and Sullivan, W. (2019). A symbiont's guide to the germline. Curr Top Dev Biol *135*, 315-351. 10.1016/bs.ctdb.2019.04.007.

Russell, S.L., Lemseffer, N., and Sullivan, W.T. (2018a). *Wolbachia* and host germline components compete for kinesin-mediated transport to the posterior pole of the *Drosophila* oocyte. PLoS Pathog *14*, e1007216. 10.1371/journal.ppat.1007216.

Russell, S.L., Lemseffer, N., White, P.M., and Sullivan, W.T. (2018b). *Wolbachia* and host germline components compete for kinesin-mediated transport to the

posterior pole of the *Drosophila* oocyte. PLoS Pathog *14*, e1007216. 10.1371/journal.ppat.1007216.

Rørth, P. (2002). Initiating and guiding migration: lessons from border cells. Trends Cell Biol *12*, 325-331. 10.1016/s0962-8924(02)02311-5.

Salzberg, S.L., Dunning Hotopp, J.C., Delcher, A.L., Pop, M., Smith, D.R., Eisen, M.B., and Nelson, W.C. (2005). Serendipitous discovery of *Wolbachia* genomes in multiple *Drosophila* species. Genome Biol *6*, R23. 10.1186/gb-2005-6-3-r23.

Sander (1968). Developmental physiological studies on embryonal mycetoma *Euscelis plebejus* I. Removal of and abnormal combination of unicellular components of symbiotic systems. 16-38.

Seemann, T. (2014). Prokka: rapid prokaryotic genome annotation. Bioinformatics *30*, 2068-2069. 10.1093/bioinformatics/btu153.

Serbus, L.R., and Sullivan, W. (2007). A cellular basis for *Wolbachia* recruitment to the host germline. PLoS Pathog *3*, e190. 10.1371/journal.ppat.0030190.

Serbus, L.R., Casper-Lindley, C., Landmann, F., and Sullivan, W. (2008). The genetics and cell biology of *Wolbachia*-host interactions. Annu Rev Genet *42*, 683-707. 10.1146/annurev.genet.41.110306.130354.

Serbus, L.R., Cha, B.J., Theurkauf, W.E., and Saxton, W.M. (2005). Dynein and the actin cytoskeleton control kinesin-driven cytoplasmic streaming in *Drosophila* oocytes. Development *132*, 3743-3752. 10.1242/dev.01956.

Serbus, L.R., Ferreccio, A., Zhukova, M., McMorris, C.L., Kiseleva, E., and Sullivan, W. (2011). A feedback loop between *Wolbachia* and the *Drosophila* gurken mRNP complex influences *Wolbachia* titer. J Cell Sci *124*, 4299-4308. 10.1242/jcs.092510.

Serbus, L.R., White, P.M., Silva, J.P., Rabe, A., Teixeira, L., Albertson, R., and Sullivan, W. (2015). The impact of host diet on *Wolbachia* titer in *Drosophila*. PLoS Pathog *11*, e1004777. 10.1371/journal.ppat.1004777.

Siggers, K.A., and Lesser, C.F. (2008). The Yeast *Saccharomyces cerevisiae*: a versatile model system for the identification and characterization of bacterial virulence proteins. Cell Host Microbe *4*, 8-15. 10.1016/j.chom.2008.06.004.

Steinhauer, J., and Kalderon, D. (2006). Microtubule polarity and axis formation in the *Drosophila* oocyte. Dev Dyn *235*, 1455-1468. 10.1002/dvdy.20770.

Sullivan, W., Ashburner, M., and Hawley, R.S. (2000). *Drosophila* Protocols. Cold Spring Harbor Press.

Sullivan W. *Wolbachia*. Bottled water, and the dark side of symbiosis. Mol Biol Cell. 2017 Sep 1;28(18):2343-2346. doi: 10.1091/mbc.E17-02-0132. PMID: 28855327; PMCID: PMC5576898.

Theurkauf, W.E., and Hazelrigg, T.I. (1998). In vivo analyses of cytoplasmic transport and cytoskeletal organization during *Drosophila* oogenesis: characterization of a multi-step anterior localization pathway. Development *125*, 3655-3666.

Theurkauf, W.E., Smiley, S., Wong, M.L., and Alberts, B.M. (1992). Reorganization of the cytoskeleton during *Drosophila* oogenesis: implications for axis specification and intercellular transport. Development *115*, 923-936.

Theurkauf, W.E. (1994). Microtubules and cytoplasm organization during *Drosophila* oogenesis. Dev Biol *165*, 352-360. 10.1006/dbio.1994.1258.

Turelli, M., and Hoffmann, A.A. (1995). Cytoplasmic incompatibility in *Drosophila* simulans: dynamics and parameter estimates from natural populations. Genetics *140*, 1319-1338.

Turelli, M., Cooper, B.S., Richardson, K.M., Ginsberg, P.S., Peckenpaugh, B., Antelope, C.X., Kim, K.J., May, M.R., Abrieux, A., Wilson, D.A., et al. (2018). Rapid Global Spread of wRi-like *Wolbachia* across Multiple *Drosophila*. Curr Biol *28*, 963-971.e968. 10.1016/j.cub.2018.02.015.

Veneti, Z., Clark, M.E., Karr, T.L., Savakis, C., and Bourtzis, K. (2004). Heads or tails: host-parasite interactions in the *Drosophila-Wolbachia* system. Appl Environ Microbiol *70*, 5366-5372. 10.1128/AEM.70.9.5366-5372.2004.

Werren, J.H., Baldo, L., and Clark, M.E. (2008). *Wolbachia*: master manipulators of invertebrate biology. Nat Rev Microbiol *6*, 741-751. 10.1038/nrmicro1969.

White, P.M., Serbus, L.R., Debec, A., Codina, A., Bray, W., Guichet, A., Lokey, R.S., and Sullivan, W. (2017). Reliance of *Wolbachia* on High Rates of Host Proteolysis Revealed by a Genome-Wide RNAi Screen of *Drosophila* Cells. Genetics *205*, 1473-1488. 10.1534/genetics.116.198903.

Wu, M., Sun, L.V., Vamathevan, J., Riegler, M., Deboy, R., Brownlie, J.C., McGraw, E.A., Martin, W., Esser, C., Ahmadinejad, N., et al. (2004). Phylogenomics of the reproductive parasite *Wolbachia* pipientis wMel: a streamlined genome overrun by mobile genetic elements. PLoS Biol *2*, E69. 10.1371/journal.pbio.0020069.

Yen, J., Barr, A. New Hypothesis of the Cause of Cytoplasmic Incompatibility in *Culex pipiens* L. *Nature* 232, 657–658 (1971). https://doi.org/10.1038/232657a0